Verediana Massa
Licenciada em Biotecnologia

Identification of prognostic biomarkers of cortical stroke in mouse model

Dissertação para obtenção do Grau de Mestre em
Genética Molecular e Biomedicina

Orientador: Professor Doutor Matteo Caleo, Instituto de Neurociência, CNR

Co-orientador: Doutora Claudia Alia, Instituto de Neurociência, CNR

Presidente: Doutor José Paulo Nunes de Sousa Sampaio

Vogal: Doutora Paula Maria Theriaga Mendes Bernardes Gonçalves

Arguente: Doutora Margarida Casal Ribeiro Castro Caldas Braga

FACULDADE DE CIÊNCIAS E TECNOLOGIA
UNIVERSIDADE NOVA DE LISBOA

Setembro 2019

Verediana Massa
Licenciada em Biotecnologia

Identification of prognostic biomarkers of cortical stroke in mouse model

Dissertação para obtenção do Grau de Mestre em Genética Molecular e Biomedicina,
Faculdade de Ciências e Tecnologia, Universidade Nova de Lisboa

Orientadores: Matteo Caleo e Claudia Alia

Setembro 2019

Identification of prognostic biomarkers of cortical stroke in mouse model

Copyright © Verediana Massa, Faculdade de Ciências e Tecnologia, Universidade Nova de Lisboa

A Faculdade de Ciências e Tecnologia e a Universidade Nova de Lisboa têm o direito, perpétuo e sem limites geográficos, de arquivar e publicar esta dissertação através de exemplares impressos reproduzidos em papel ou de forma digital, ou por qualquer outro meio conhecido ou que venha a ser inventado, e de divulgar através de repositórios científicos e de admitir a sua cópia e distribuição com objetivos educacionais ou de investigação, não comerciais, desde que seja dado crédito ao autor e editor.

Abstract

According to the *World Health Organization* (WHO), worldwide, 15 million people suffer stroke each year. Stroke, i.e. the sudden and severe reduction of blood flow to a brain region, is the second leading cause of death and the third leading cause of disability. Stroke is also a leading cause of dementia and depression. A focal brain damage inevitably causes a drastic alteration of the whole complex neural network that characterizes the affected area. Although stroke damage can be devastating, many patients survive the initial event and display a spontaneous recovery, which can be further increased by rehabilitation therapy. Recovery is possible due to a reorganization of spared areas and connections, i.e. neuroplasticity.

Functional recovery is highly variable in stroke patients and strongly depends on many factors (lesion location and volume, etc.). Currently, there are no ways of predicting either the degree or time course of recovery in individual subjects. For these reasons, the identification of biomarkers is crucial in the design and interpretation of stroke rehabilitation trials. Therefore, the aim of this work is the development of new prognostic and therapeutic tools in preclinical models.

In this study I exploit a mouse model of stroke, the Middle cerebral artery occlusion (MCAO), that shows a higher variability and is thus closer to the human condition. I conducted experiments to evaluate the occurrence of motor deficits using a battery of behavioral tasks: gridwalk test, skilled reaching test, and retraction task in the M-platform (a robotic device that permits to quantitatively evaluate several kinetic/kinematic parameters related to forelimb movement). Moreover, the ischaemic lesion and electrophysiological alterations was analysed by means of histology and electroencephalographic signals (EEG) respectively. I studied how these mechanisms are altered by stroke, combining the data all these parameters, in order to define possible biomarkers that predict long-term motor recovery.

The results obtained, permit new opportunities for therapeutic approaches after stroke allowing the definition of more effective rehabilitation paradigms that can be translated into clinical practice.

Keywords: Stroke, Middle Cerebral Artery, Biomarkers, Recovery, Motor functional

Sumário

Segundo a Organização Mundial da Saúde (OMS), no mundo todo, 15 milhões de pessoas sofrem de Acidente Vascular Cerebral (AVC) a cada ano. AVC, nomeadamente, a redução súbita e severa do fluxo sanguíneo para uma região cerebral, é a segunda principal causa de morte e a terceira principal causa de incapacidade. O AVC também é uma das principais causas de demência e depressão. Um dano cerebral focal inevitavelmente causa uma alteração drástica de toda a complexa rede neural que caracteriza a área afetada. Embora o dano por AVC possa ser devastador, muitos pacientes sobrevivem ao evento inicial e apresentam uma recuperação espontânea, que pode ser aumentada pela terapia de reabilitação. A recuperação é possível devido a uma reorganização de áreas e conexões poupadas, ou seja, a neuroplasticidade. A recuperação funcional é altamente variável em pacientes com AVC e depende fortemente de muitos fatores (localização e volume da lesão, etc.). Atualmente, não há maneiras de prever o grau ou o decurso da recuperação individual. Por essas razões, a identificação de biomarcadores é crucial no desenho e interpretação de estudos de reabilitação de AVCs. Portanto, o objetivo deste trabalho é o desenvolvimento de novas ferramentas prognósticas e terapêuticas em modelos pré-clínicos.

Neste estudo exploro um modelo em murganho de AVC, a oclusão da artéria cerebral média (MCAO), que mostra uma maior variabilidade e, portanto, está mais próximo da condição humana.
Conduzi experimentos para avaliar a ocorrência de déficits motores utilizando uma bateria de tarefas comportamentais: gridwalk test, teste de alcance qualificado e tarefa de retração na plataforma M (um dispositivo robótico que permite avaliar quantitativamente vários parâmetros cinéticos/quinemáticos relacionados ao movimento dos membros anteriores).
Para além disso, a lesão isquêmica e as alterações eletrofisiológicas foram analisadas por meio de histologia e sinais eletroencefalográficos (EEG), respectivamente. Estudei como esses mecanismos são alterados pelo AVC, combinando os dados obtidos, a fim de definir possíveis biomarcadores que prevêem a recuperação motoria a longo prazo.

Os resultados obtidos, consentem novas oportunidades de abordagens terapêuticas após AVC, permitindo a definição de paradigmas de reabilitação mais eficazes, que podem ser traduzidos na prática clínica.

Palavras-chave: Acidente Vascular Cerebral (AVC), Artéria Cerebral Média, Biomarcadores, Recuperação, Função motoria

Table of Contents

Abstract ..... **i**

Sumário ..... **iii**

Table of Contents ..... **v**

Figure index ..... **vii**

Abbreviation and Symbols ..... **ix**

Chapter 1. Introduction **1**

1.1 Stroke Description 1

1.1.1 Historical references 1

1.1.2 Definition and Symptoms 2

1.1.3 Hemorrhagic/ischemic stroke 2

1.1.4 Incidence 5

1.1.5 Risk factors 5

1.1.6 Effects in Nervous System 5

1.2 Animal Model 7

1.2.1 Focal cerebral ischaemia model 7

1.2.2 Middle cerebral artery occlusion (MCAO) 9

1.2.3 Permanent electrocoagulation model of MCAO 10

1.3 Post-stroke Rearrangements 11

1.3.1 Spontaneous recovery 11

1.3.2 Proportional recovery rule 12

1.3.3 Clinical outcomes 12

1.4 Biomarkers of Stroke Recovery 13

1.4.1 Measures of motor function 13

1.4.2 Measures of anatomical/structural injury 15

1.4.3 Combined approaches 16

1.5 Aims of the study 17

Chapter 2. Materials and Methods **19**

2.1 Experimental design 19

2.2 Electrode Implant 19

2.3 Permanent Middle Cerebral Artery Occlusion 20

2.4 Immunohistochemistry 21

2.5 Anatomical/structural measures 21

2.5.1 Lesion volume and CFA integrity 21

2.5.2 White matter integrity 23

2.6 Behavioural tests 24

2.6.1 Reaching test..... 24
2.6.2 Gridwalk test..... 24
2.6.3 Robot task..... 25
2.6.4 Motor score..... 26
2.6.5 Statistical Analysis..... 27
2.7 Neurophysiological recordings..... 27
2.7.1 Electrophysiology in free moving..... 27
2.7.2 Electrophysiology onto the robotic platform..... 27
Chapter 3. Results..... 29
3.1 Post-stroke anatomical alterations..... 29
3.1.1 Lesion volume and cortical integrity..... 29
3.1.2 White matter integrity..... 31
3.2 Alterations in motor function after MCAO..... 32
3.3 Proportional recovery in MCAO model..... 37
3.4 Preliminary correlation between functional and anatomical changes..... 38
3.5 Electrophysiological alterations after MCAO..... 39
3.5.1 MCAO-induced power spectral density changes..... 39
3.5.2 Preliminary evaluation of electrophysiological changes in the M-plattaform..... 41
Chapter 4. Discussion..... 43
4.1 Anatomical and behavioural changes in MCAO induction 43
4.2 Proportional recovery and preliminary correlation analysis..... 44
4.3 Post-stroke electrophysiological alterations..... 45
References..... 47

Figure index

Figure 1.1 – Figure depicts an historical timeline..... 2
Figure 1.2 – Subtypes of stroke..... 3
Figure 1.3 – Types of hemorrhagic stroke..... 3
Figure 1.4 – Types of ischemic stroke..... 4
Figure 1.5 – Structure of microvacuolated hippocampal neuron..... 6
Figure 1.6 – Signalling pathways involved in the cerebral ischemic cascade..... 8
Figure 1.7 – Comparison of somatosensory and motor areas in primates and rodents..... 9
Figure 1.8 – Circle of Willis..... 10
Figure 1.9 – Middle cerebral artery..... 10
Figure 1.10 – Cross section rodent cortex that shows the stroke core and penumbra..... 10
Figure 1.11 – Different recovery curves of patients with initially severe upper limb impairment..... 12

Figure 2.1 – Timeline of experiments..... 19
Figure 2.2 – Location of EEG electrodes..... 20
Figure 2.3 – Measures considered after stroke..... 21
Figure 2.4 – Lesioned CFA..... 22
Figure 2.5 – Example of shrinkage and distortion..... 23
Figure 2.6 – White matter assessments..... 24
Figure 2.7 – Behavioural tests..... 25
Figure 2.8 – M-Platform..... 26

Figure 3.1 – Histological brain slices at 30dpl..... 29
Figure 3.2 – NeuN staining of at bregma level 0 in six different MCAO animals 30dpl..... 30
Figure 3.3 – Ipsilesional cortical shrinkage at 30dpl..... 30
Figure 3.4 – CFA lesion on 30dpl histological brain slice..... 31
Figure 3.5 – Histological brain slice stained with Luxol fast blue protocol..... 31
Figure 3.6 – Ipsi/Contra ratio of white matter integrity..... 32
Figure 3.7 – Analysis of skilled reaching test performance..... 33
Figure 3.8 – Analysis of gridwalk test performance..... 34
Figure 3.9 – Analysis of robot task performance..... 34
Figure 3.10 – Analysis of isometric performance..... 35
Figure 3.11 – Motor score..... 36
Figure 3.12 – Motor score sum..... 37
Figure 3.13 – Recovery trend in MCAO group..... 37
Figure 3.14 – Acute deficit trend in MCAO group..... 38
Figure 3.15 – Linear regression between reaching test and lesion volume..... 38
Figure 3.16 – Linear regression between reaching test and CFA lesioned mice..... 39
Figure 3.17 – Linear regression between isometric task and CFA, volume lesioned mice..... 39

Figure 3.18 – EEG power spectral density changes after MCAO induction..... 40
Figure 3.19 – EEG power spectral density changes in MCAO group..... 40
Figure 3.20 – Post-stroke evolution of electrophysiological parameters..... 41

Abbreviations and symbols

Abbreviation

ADL – Activity of daily living
AMPA – α-amino-3-hydroxy-5-methyl-4-isoxazolepropionic acid receptor
ATP – Adenosine triphosphate
AUC – Area under the curve
CFA – Caudal forelimb area
CST – Corticospinal tract
CT – Computerized tomography
DALYs – Disability-adjusted life years
DNA – Deoxyribonucleic acid
Dpl – Days post-lesion
DTI – Diffusion tensor imaging
DW-MRI – Diffusion-weighted magnetic resonance imaging
EEG – Electroencephalographic
ERP – Event-related potential
fMRI – Functional magnetic resonance imaging
ICA – Internal carotid artery
IL-1β – Interleukin 1β
LFP – Local field potentials
M1 – Primary motor cortex
MCA – Middle cerebral artery
MCAO – Middle cerebral artery occlusion
MEG – Magnetoencephalography
MRBD – Movement-related beta desynchronization
MRI – Magnetic resonance imaging
NIHSS – National Institutes of Health Stroke Scale
NMDA – N-methyl-D-aspartate
PBS – Phosphate buffered saline
PFA – Paraformaldehyde
PMd – Dorsal premotor cortex
PREP Predicting recovery potential
ROS – Reactive oxygen species
rsFC – Functional connectivity of the resting state
S1 – Primary somatosensory cortex
SAFE – Survey on the access to finance of enterprises
SMA – Supplementary motor area
TIA – Transient ischaemic attack

TNFα – Tumor necrosis factor α
WHO – World Health Organization
WSO – World Stroke Organization

Symbols

* - Times
/ - Divided
% - Percentage
°C – Degrees Celsius
+ - Plus
> - Major
~ - Circa
cm – Centimeter
cm – Centimetre
g – Grams
h – Hour
Hz – Hertz
mg/kg – Milligram per kilogram
ml/kg – Milliliter per kilogram
mm – Millimetre
s – Second
W – Watt
µm – Micrometre

Chapter 1. Introduction

1.1 Stroke Description

1.1.1 Historical references

The first use of the term "stroke" was in 1599, attributing the sudden appearance of symptoms to a ‘stroke of God’s hand’ (Pound et al., 1997). It was not adopted into the medical lexicon of the time and the doctors used the term “apoplexy”, a diagnosis that had been in existence since the Hippocratic writings (Karenberg and Moog, 1997).

Apoplexy was a generic term, which describes a condition in which the patient had a sudden abolition of all the activities of the mind with the preservation of the pulse and breathing. Hippocrates described a patient who experiences sudden pain, loses his speech, with a gasp in the throat, urine without awareness and does not respond (Pound et al., 1997).

In the Hippocratic writings, the word used to describe such results was "paraplessia" and, although now obsolete, is meant as a synonym for what we now define "paraplegia" (Coupland et al., 2017).

It was only in the seventeenth century and the rise of the anatomical doctors that this position was challenged. Among the most important advances in stroke comprehension were those made by the physician Johan Jakob Wepfer. Wepfer is credited with being the first to observe that apoplexy was caused by an intracranial haemorrhage (Pound et al., 1997).

Over time, the number of autopsies performed has increased and the most significant work published in the 17th century was the *Sepulchretum sive* of *Anophetic Practica* by Theophile Bonet.

Bonet's *Sepulchretum* was much appreciated, but was eventually replaced by the publication of *De Sedibus* et *Causis Morborum per Anatomen Indagatis* by Giovoanni Morgagni in 1761. Morgagni, considered to be the founder of pathology, built on Bonet’s work but with fundamental differences: he did not recognize cranial trauma as a cause of apoplexy (although he admitted that he could cause a "apoptotic condition") and divided the causes of apoplexy into two main groups: "sanguineous" and "serous" (Schutta, 2009).

With such observations, apoplexy began to be understood as a predominantly vascular disease, a position strengthened by the discoveries of John Abercrombie (early 19th century) and Rudolf Virchow (early 20th century). The first recognized a link between arterial occlusive disease and areas of cerebral softening (caused by infarcts) and the latter reclassified the causes of apoplexy as sanguinea (hemorrhagic) and ischemia (Virchow term) (Coupland, 2017). So the term “cerebrovascular disease” emerged and apoplexy faded from use (**Figure. 1.1**).

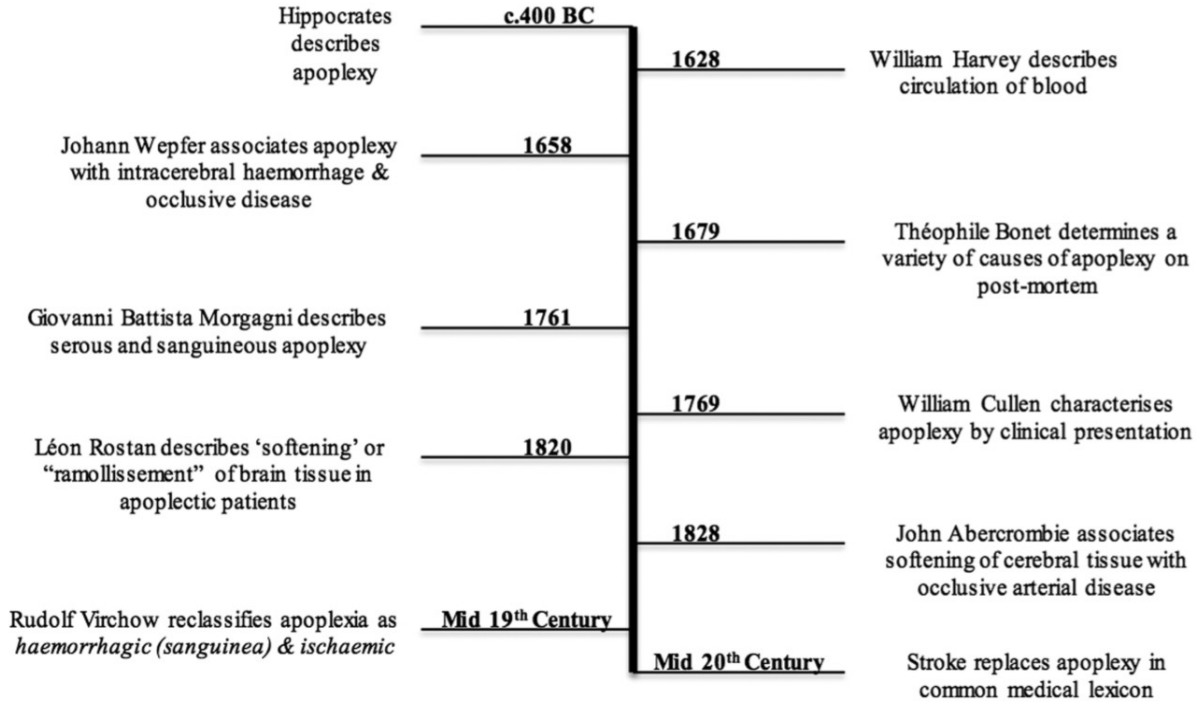

Figure1. 1: Figure depicts an historical timeline *(*Coupland et al., 2017*).*

1.1.2 Definition and Symptoms

In 1970, the World Health Organization (WHO) defined stroke as "rapidly developed clinical signs of focal (or global) disturbance of cerebral function, lasting more than 24 hours or leading to death, with no apparent cause other than of vascular origin" (Aho et al., 1980). Although still widely used, the definition of the World Health Organization is strongly based on clinical symptoms and is now considered obsolete by the American Heart Association and the American Stroke Association due to significant advances in nature, timing, and stroke recognition. Today the most current definition provided by WHO is: "A stroke is caused by the interruption of the blood supply to the brain, usually because a blood vessel bursts or is blocked by a clot. This cuts off the supply of oxygen and nutrients, causing damage to the brain tissue."

Typical stroke symptoms include sudden unilateral weakness, numbness or visual loss, impaired speech, ataxia and vertigo. Associated symptoms (e.g. headaches) vary and usually reflect the cause or consequences of stroke. Atypical symptoms include isolated vertigo, binocular blindness, amnesia, stridor, alien hand syndrome, confusion, and altered consciousness (Coupland et al., 2017).

1.1.3 Hemorrhagic/ischemic stroke

Pathological subtypes of stroke include: ischemic stroke (cerebral infarction) and hemorrhagic stroke (intra-cerebral hemorrhage and subarachnoid hemorrhage). The proportions of pathological and aetiological subtypes of stroke varies among populations, in relation to age, nationality and nation lifestyle. Ischemia is characterized by an insufficient blood supply **(Figure. 1.2 A)**, while hemorrhage is characterized by an excess of blood inside the skull **(Figure. 1.2 B)**.

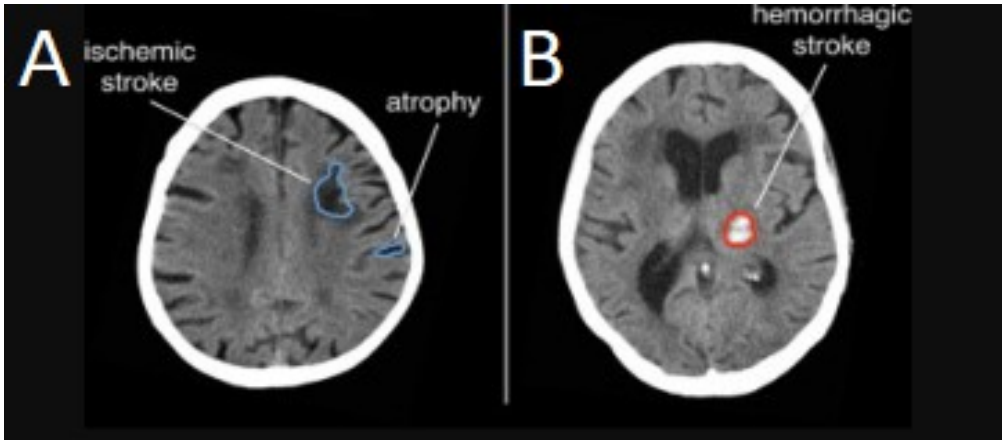

Figure1. 2: Subtypes of stroke. (A) *Ischemic stroke;* ***(B)*** *Hemorrhagic stroke. (*Gillbert et al., 2014)

Hemorrhagic stroke refers to bleeding inside the skull either in the brain or at the level of the meninges. Bleeding in the brain parenchyma or vascular system produces an impairment in the intracerebral connections and in the pathway of gray and white matters. This bleeding is due to the rupture of small blood vessels, arterioles and capillaries in the cerebral parenchyma, and therefore, blood oozes into the brain and forms a localized blood collection called hematoma. When hematoma is formed, it exerts pressure on the regions of the brain and can injure these surrounding tissues.

Edema often develops around the hematoma, further adding to the extra volume of abnormal tissue. Large hemorrhages are usually fatal because they increase pressure within the skull, squeezing vital regions in the brainstem.

Bleeding into the fluid around the brain is referred to as subarachnoid hemorrhage, in which the blood collects under the arachnoid membrane that lies over the pia mater. In contrast to the situation in intra-cerebral hemorrhages, where a localized hematoma causes loss of function related to a specific area **(Figure. 1.3)**, in patients with subarachnoid hemorrhages there are more systemic symptoms (e.g. headache, vomiting, seizures, decreased consciousness, etc.) (Van Gijn et al., 2007).

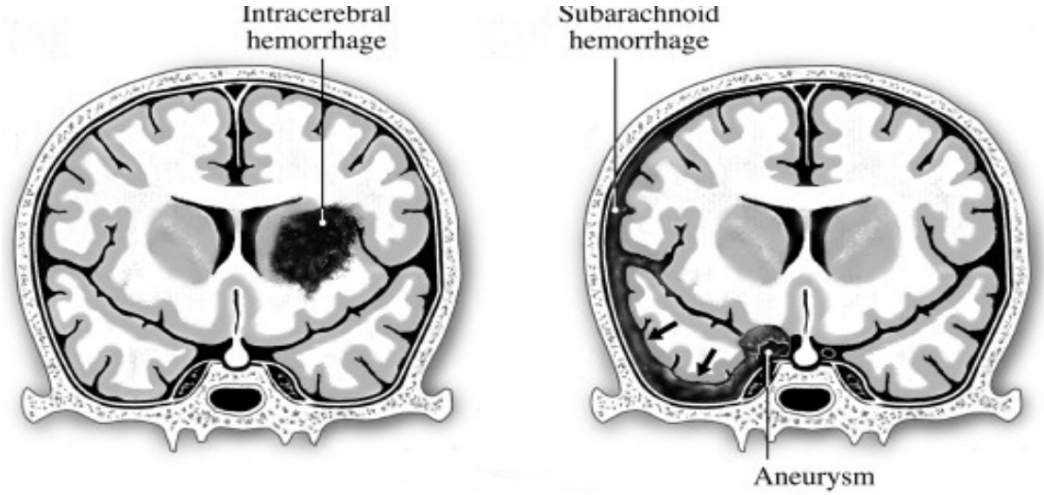

Figure1. 3: Types of hemorrhagic stroke *(*Caplan and Simon, 2015*).*

The second main types of stroke are ischemic (Amarenco et al., 2009). The term refers to the insufficiency of blood supply to an organ.

There are three main categories of cerebral ischemia, called: thrombosis, embolism and systemic hypo-perfusion **(Figure. 1.4).** Each one indicates a different mechanism of lesion of blood vessels or a reason of decreased blood flow.

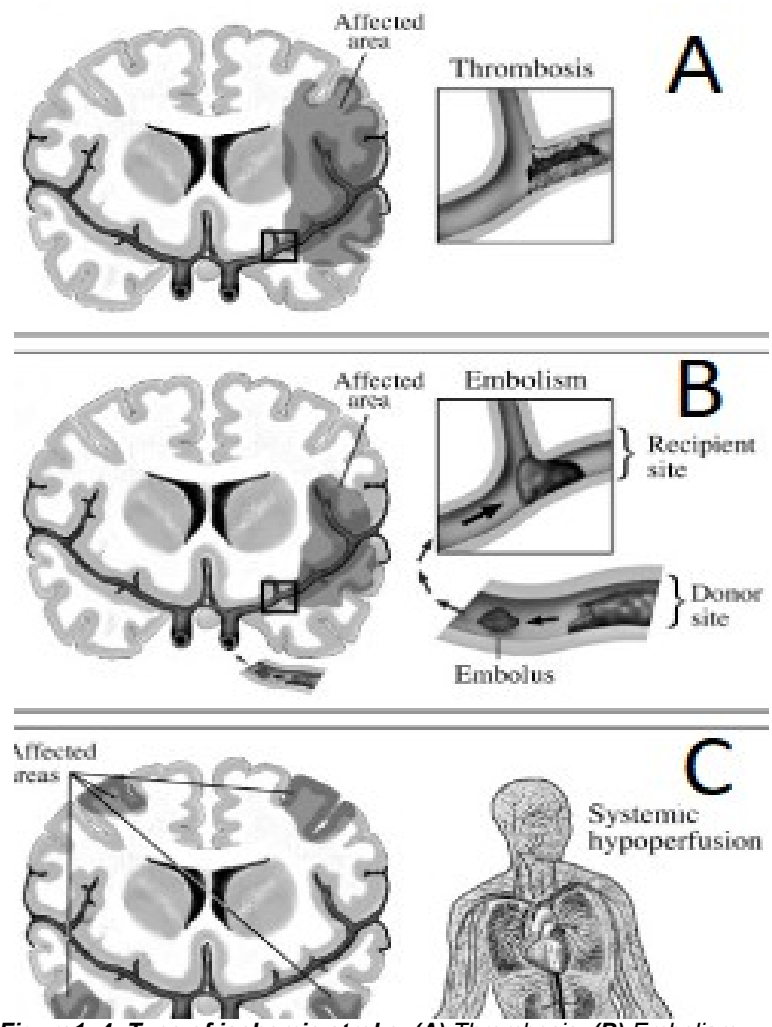

Figure1. 4: Type of ischemic stroke. (A) *Thrombosis;* ***(B)*** *Embolism;* ***(C)*** *Systemic Hypoperfusion. (*Caplan and Simon, 2015*).*

Thrombosis refers to a local problem within a blood vessel that supplies a portion of the brain. The process is often a disease of the blood vessel, which narrows blood flow through that vessel. Often, a thrombus is superimposed on the localized vascular process. Embolism refers to a breaking loose of materials (often thrombi, but occasionally bacteria, cholesterol crystals, fat, foreign bodies, etc.) from a proximal source to block a distant vessel farther along the circulatory path. The downstream blocked vessel causes infarction to a localized brain region in the same way that a primary vascular lesion (i.e. thrombosis) does. Systemic hypoperfusion is characterized by a global decrease in blood flow to the head rather than a localized decrease as occurs in thrombosis and embolism. Abnormal heart performance could lead to low pressure in the cardiovascular system.

Abnormally slow or fast heart rhythms, cardiac arrest and heart failure can reduce blood flow to the head and brain. Another cause of decreased circulatory function is a lowering of blood pressure and blood flow due to an inadequate amount of blood and fluid in the vascular compartment of the body. Bleeding, dehydration and fluid loss in body tissues (shock) can lead to inadequate brain failure.

1.1.4 Incidence

Stroke is the second leading cause of death and the third leading cause of disability (WHO). Worldwide, 15 million people suffer stroke each year, of these, 5 million die and another 5 million are permanently disabled. Current trends suggest that the number of annual deaths will rise to 6.7 million (World Stroke Organization (WSO)).

Globally, men continue to have a higher incidence of ischemic stroke than women, while no significant gender differences were observed in the incidence of hemorrhagic stroke (Barker-Collo et al., 2015). It is possible that the differences between men and women are partialy explained by the fact that in some countries women are more sensitive to health information, have a more healthy behaviour and have better access to primary prevention. An alternative explanation is that the neurovascular risk factors are more frequent and severe in men and have decreased more rapidly in women (e.g. the differential rate of smoking, with men having a higher prevalence of smoking than women). The total health loss due to stroke as measured by Disability-adjusted life years (DALYs) is similar for men and women for both stroke subtypes.

The increasing incidence and mortality rates of ischaemic stroke in the last decades represent a significant improvement in the health of the population and is observed for both sexes and in all groups of age. These significant improvements are concomitant with interventions for a better prevention of cardiovascular risks.

According to the statistics of SAFE, in Portugal the incidence is 15.208 strokes per year, i.e., each year, in 1000 people, approximately 2 suffer a stroke and 41% of stroke survivors are unable. From 2015 to 2035 the estimated increase in incidence is 31%, with a fatal increase of 40% and DALY loss of 29% (The Burden of Stroke in Europe, 2017).

1.1.5 Risk factors

Hypertension, hypercholesterolaemia, carotid stenosis and atrial fibrillation are known to be risk factors for stroke because clinical studies have shown that treating these conditions reduces stroke (Xie et al., 2016). Cigarette smoking, excessive alcohol use, insulin resistance and diabetes mellitus are also likely to be risk factors. O ther comorbidity factors are represented by environmental air pollution, health condition, high risk diet and poor nutrition, physical inactivity, obesity, ageing, variability of blood pressure, disordered breathing of sleep, chronic inflammation, chronic kidney disease, headache, depression, stress, long hours of work. These factors, if modified, could reduce stroke incidence.

1.1.6 Effects in Nervous System

Global ischemia produces the non-focal cessation of blood flow to the entire brain, as happens in cardiac arrest. Energy deficiency from impaired oxidative metabolism occurs rapidly when substrates for adenosine triphosphate (ATP), oxygen and glucose decrease. Neuronal injury and cell death begin within 4 minutes. The distinctive morphological sign of the neuronal lesion is the change of ischaemic cells characterized by microvacuolization in the cytoplasm (Song and Yu, 2014). At ultrastructural level, the vacuoles mainly represent dilated mitochondria with Ca2+ loading (**Figure. 1.5**).

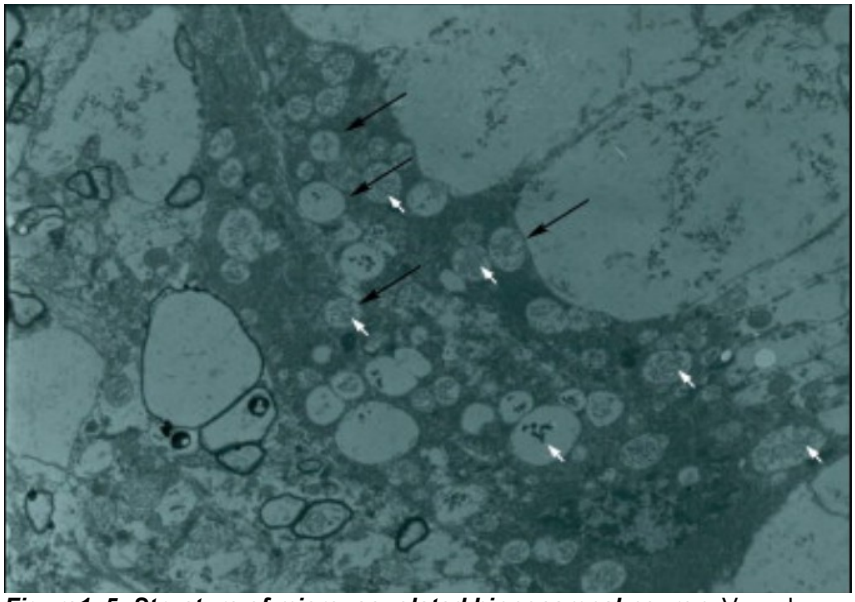

Figure1. 5: Structure of microvacuolated hippocampal neuron. Vacuoles, black arrows, are dilated mitochondria which show calcium deposits, white arrows (Caplan and Simon, 2015).

Focal ischemia produces an altered blood flow in a portion of the brain as occurs in thrombotic and embolic strokes. Here, there is a decrease of energy, more in the ischaemic core than in the surrounding cerebral tissue, referred to as “penumbra” (Arumugam et al., 2018). Na + / K + -ATPase, responsible for maintaining the intracellular concentration of K+, fails, resulting in loss of K+ and consequent excessive depolarization of downstream neurons. This produces a cortical depression, producing further neuronal and astrocytic depolarization and infarct extension. Cellular depolarization causes intracellular Ca2+ entry through activation of voltage-gated Ca2+ channels and voltage-sensitive glutamate receptor-gated channels. Anaerobic metabolism causes lactate accumulation and acidosis in regions of the ischaemic brain. The presence of acidosis activates Ca2+-permeable, acid-sensing ion channels, further exacerbating calcium dysregulation. Intracellular Ca2+ buffering and sequestration mechanisms in mitochondria and endoplasmic reticulum become overwhelmed catabolic processes are activated, mitochondrial function fails, and cell death pathways are mobilized.

Cell death occurs more rapidly in the infarct core and more slowly (after several hours or days) in the penumbra (Caplan and Simon, 2015). Rapid cell death occurs through the process of necrosis, with swelling of cells and organelles, breakage of the membrane and leakage of cellular content into the extracellular space with consequent inflammation. The swelling of the organelles results in cytoplasmic microvacuolysis. In the penumbra, cell death occurs in a slower, more energy-dependent and more regulated way, characterized by programmed cell death. Here, in contrast to necrosis, the affected cells are characterized by shrinkage, membrane blebbing without breakage, aggregation of the chromatin on the nuclear membrane, preservation of the integrity of intracellular organelles with subsequent dispersion of the cellular content in apoptotic bodies bound to the membrane and finally fragmentation of the DNA. In this case, inflammation does not result.

Several pathways contribute and facilitate cell death. Excitotoxicity refers to the pathological effect of excitatory neurotransmitters, in particular glutamate, which is present in high concentrations in the extracellular space of the ischaemic brain. The increased glutamate concentration produce depolarization-induced synaptic release, reversal of astrocytic glutamate uptake, and activation of voltage-sensitive glutamate receptor-gated channels. Extracellular glutamate binds to the postsynaptic

N-methyl-D-aspartate (NMDA) receptor, in particular the extrasynaptic receptors containing an NR2B subunit. The NMDA receptor gates a Ca2+-permeable ion channel and its activation produces a further influx of Ca2+. Moreover, the entry of Ca2+ from this path leads to the activation of the neuronal nitric oxide synthase, resulting in the production of reactive oxygen species (ROS) that produce mitochondrial and DNA damage, ion channel activation, protein modification and activation of cell death paths.

The Ca2+ released increases free radicals, triggers the expression of a number of proinflammatory genes by inducing the synthesis of transcription factors (e.g. interferon regulatory factor 1). Therefore, inflammation mediators, such as tumor necrosis factor α (TNFα) and interleukin 1β (IL-1β), are produced by injured brain cells. As a consequence, the expression of adhesion molecules is induced on the surface of endothelial cells, where they interact with the complementary surface receptors on neutrophils. Neutrophils, in turn, adhere to the endothelium, cross the vascular wall and enter the brain parenchyma. Macrophages and monocytes follow neutrophils, migrating into the ischaemic brain and, five or seven days after ischaemia, becoming the predominant cells. Chemokines (e.g. interleukin 8) are produced in the injured brain and drive the migration of the inflammatory cells within the blood to their target together with resident brain cells that are also involved in the inflammatory response. From four to six hours after ischaemia, astrocytes become hypertrophic, while microglial cells assume a tipical amoeboid morphology of activated microglia. Twenty-four hours after the occlusion, the microglial reaction is predominant in the ischaemic brain, leading to an increasing inflammation that contributes to brain damage, and finally, to the impairment of sensory and motor function **(Figure. 1.6)**.

1.2 Animal Model

1.2.1 Focal cerebral ischemia model

Several animal models have been developed in the recent years to study molecular and cellular mechanisms following a focal ischaemic insult in the brain and to evaluate possible therapeutic approaches for the restoration of function. In particular, rodent models allow a coordinated electrophysiological, behavioural, biochemical, and anatomical analysis of post stroke modifications. At the same time, small animals are relatively low expensive, they are easy to obtain and they can be maintained for longer periods of time. These reasons, make rodents a reasonably good model for understanding the changes in the intra-cortical communications following a brain injury.

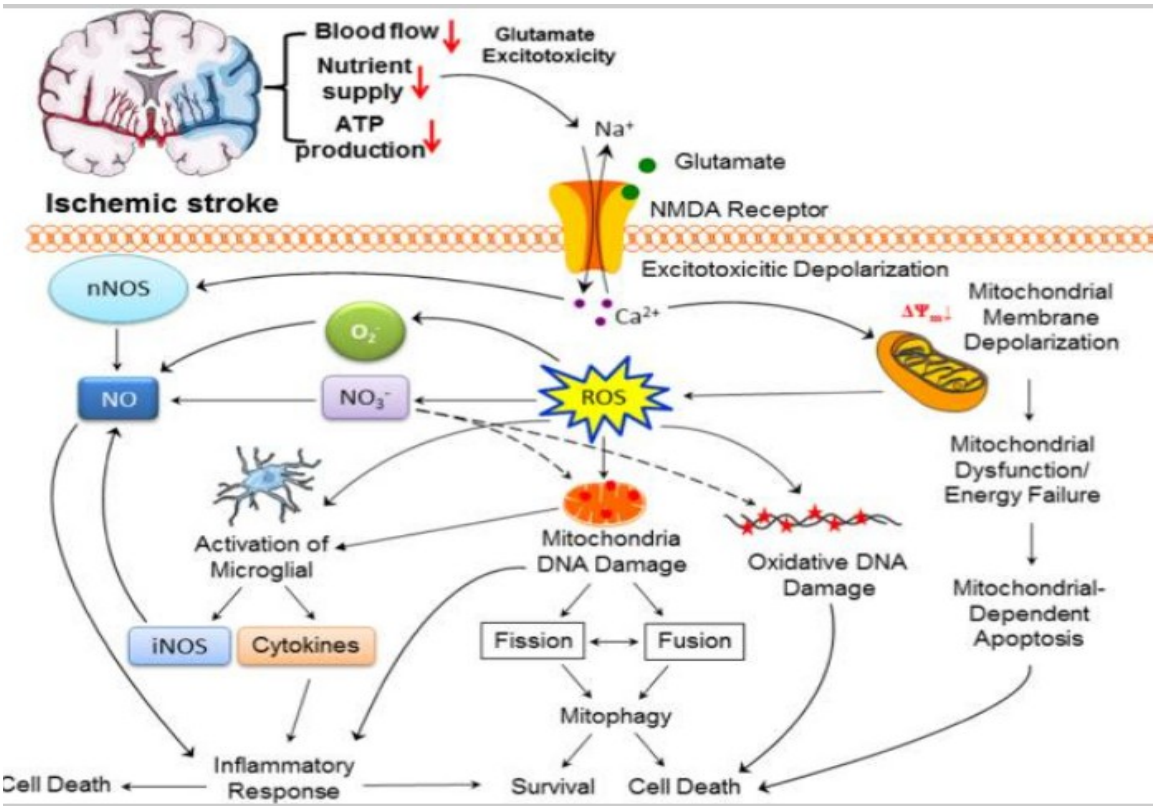

Figure1. 6: Signalling pathways involved in the cerebral ischemic cascade *(Yang et al., 2018).*

Of course, animal models that reproduce human stroke have several limitations, some of which are difficult to overcome. The human clinical stroke is often a result of a number of predisposing factors such as depression, diabetes, obesity and circulatory problems. In the animal models, stroke is induced in young and healthy individuals and in strictly controlled experimental conditions, that cannot reproduce the complexity and heterogeneity of a human stroke.

Moreover, there are differences between mammalian species and the anatomy of the tract. Primates present a higher number of corticospinal neurons than the rodents and a large number of corticospinal fibres represent a major volume of white matter in the internal capsule of primates compared with rodents.

The corticospinal tract (CST) is the main descending pathway from the cerebral cortex to spinal cord motorneurons and its cortical territories and/or fibre tracts are usually injured in stroke. Despite some differences in the CST anatomy among mammalians species, in all of them, the CST originates from layer V pyramidal neurons in the cerebral cortex. Most of corticospinal neurons are localized in a large region of frontoparietal cortex corresponding to primary motor cortex (M1) and primary somatosensory cortex (S1). Moreover, in all mammalians, the corticospinal fibres descend across the internal capsule and medullary pyramids, suggesting that, this pathways emerged early in mammalian evolution (Nudo, 2007). To the contrary, there are some difference in the proportion of crossing CST fibers. In fact, in primate fibres that cross to the contralateral side of the spinal cord prevail, while in rodents the ipsilateral component is greater and represents a potential compensatory pathway. Also for this reason, rodents often show a better and faster recovery after injury with respect to humans.

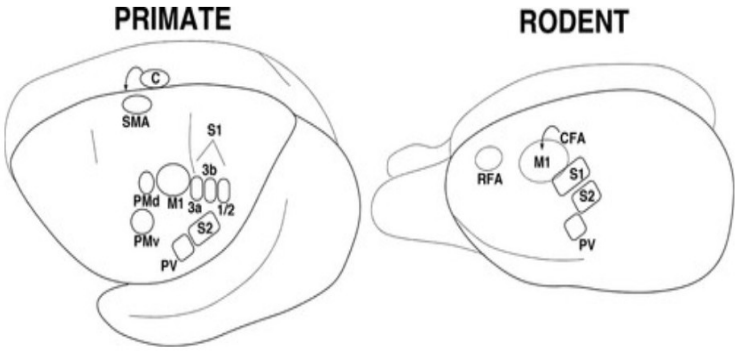

Figure1. 7: Comparison of somatosensory and motor areas in primates and rodents *(Nudo, 2007).*

In all mammalian species, including all rodents and primates, the motor and somatosensory cortices shows a topographic arrangement, with at least 2 somatosensory representations (S1 and S2), that have been identified in the parietal cortex. However, in primates, S1 can be subdivided into additional areas, including areas 3a, 3b, 1, and 2. In rodents, a primary and a putative premotor cortex have been identified, in particular regarding the forelimb motor representation, using intracortical microstimulation experiments, a caudal and rostral forelimb area (CFA and RFA respectivey) have been described (Tennant, 2010). In primates, frontal cortex has been subdivided into >5 regions including M1, supplementary motor area (SMA), ventral premotor cortex (PMv), dorsal premotor cortex (PMd), and cingulate motor areas. Each of these areas has been further subdivided into subfields (such as SMA proper and pre-SMA) **(Figure. 1.7)**

1.2.2 Middle cerebral artery occlusion (MCAO)

In humans, ischemic strokes occur more often in the brain region provided by the middle cerebral arteries (MCAs). The MCAs are relatively large cerebral arteries arising from the circle of Willis **(Figure. 1.8)**, and the occlusion of one of these arteries produces a large area of ischaemic damage and neuronal death (Dorrance and Fink, 2015). The MCA is one of the major arteries that provides blood supply to the brain. In humans, it arises from the bifurcation of the ICA (internal carotid artery) as the larger and more direct branch. It is divided into three segments: M1 is the horizontal segment, M2 is the insular segment, M3 is the opercular segment **(Figure. 1.9)**. The right and left MCAs are connected to the anterior cerebral arteries and the posterior communicating arteries, which connect to the posterior cerebral arteries, creating the Circle of Willis.

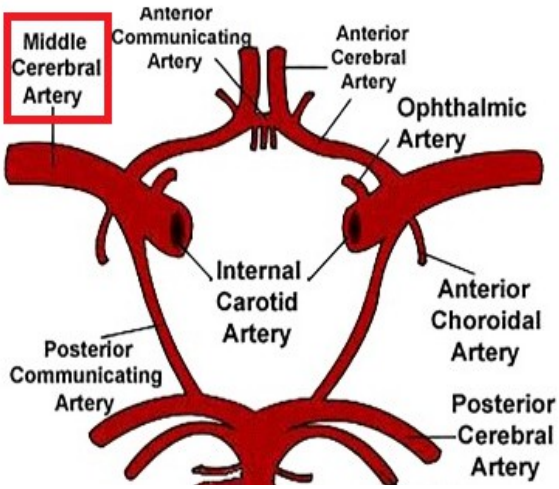

Figure1. 8: Circle of Willis *(*Wang et al., 2016*).*

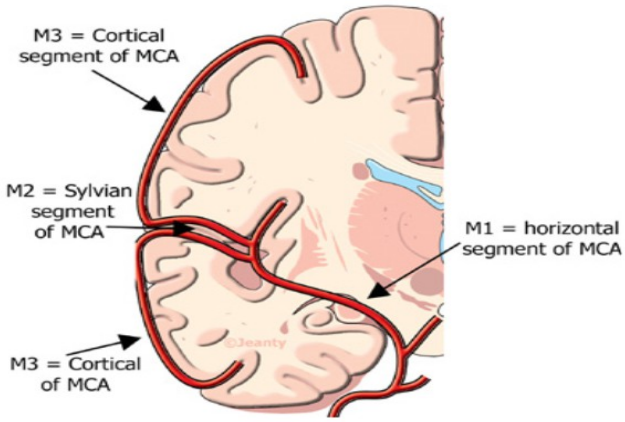

Figure1. 9: Middle cerebral artery (MCA) *(Cerekja et al., 2011).*

The middle cerebral artery occlusion (MCAO) model is widely used for inducing a focal cerebral ischemic stroke in rodents. To study the lesion, MCAO can be performed via transient or permanent model. Regarding transient model, MCAO is achieved through insertion of an intraluminal suture into the external carotid or common carotid artery and thus result in partial restoration of perfusion after transient MCAO. While, in the second model, blood flow is permanently occluded. This model will be described in the next section.

1.2.3 Permanent Electrocoagulation Model of MCAO

The electrocoagulation model of MCAO in rodents was developed by Tamura and colleagues (Tamura et al.,1981). In this model a craniotomy is accomplished in order to expose the MCA on the brain surface. Electrocoagulation forceps are used to coagulate a portion of MCA to permanently occlude the vessel.

After occlusion, the core has less than 20% of baseline blood flow and fails to regain its initial condition while, in the penumbra, blood flow re-increases towards the midline, as tissues in this region are supplied by other artery systems that were not blocked during the stroke (Li and Murphy, 2008) It has been showed that the dendritic arborisation follows the gradient of blood supply: in particular, going away from the core of the lesion, towards the healthy tissue, neurons are characterized by a more complex fine dendritic structure app **(Figure. 1.10)**.

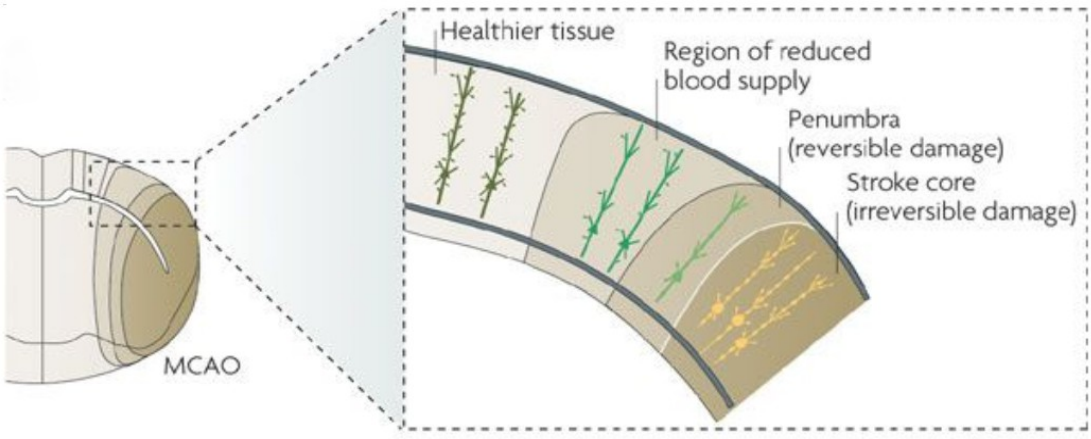

Figure1. 10: Cross section through the rodent cortex that shows the stroke core (darker brown) and penumbra (lighter brown) *(*Murphy and Corbett, 2009*).*

The advantage of this model is that the section of occluded MCA, can be varied (distal or proximal occlusion) and this can induces a stroke in cortical territory or both cortical and subcortical territories.
A distal occlusion of MCA will induce a cortical lesion, while a proximal occlusion, at the origin of MCA, will induce a great subcortical and cortical infarct.
The limitation of this model is that it induces permanently MCAO and therefore the riperfusion is not possible and due to the position of craniotomy, injury to the temporalis muscle may occur. (Tamura et al., 1981).

1.3 Post-stroke Rearrangements

1.3.1 Spontaneous recovery

A focal brain damage inevitably causes a drastic alteration of the whole complex neural network that characterizes the affected area. Although stroke damage can be devastating, many patients survive to the initial event and present a spontaneous recovery, which can be further increased by rehabilitation therapy. The destruction of neural networks, in fact, usually stimulates a rewiring and a reorganization of the connections and this plastic environment is highly sensitive to the experience following the damage (Stroemer et al., 1993; Li and Carmichael, 2006). Particularly, such phenomena involve the perilesional tissue and the surrounding brain areas of the injured hemisphere. Nevertheless, plastic phenomena can occur also in some portions of the contralateral hemisphere, as well as in subcortical and spinal regions. This window of plasticity, a sort of post-stroke critical period, appears to be time-limited and has a peak in the acute – early subacute phase. In this time window, behavioural training has its maximum effect (Biernaskie et al. 2004).
Recovery is defined by clinical and biomedical scientists as the improving of the sensory and motor performance that occurs after the stroke (Murphy and Corbett, 2009), although the re-emerging post-stroke behaviour is probably not identical to pre-stroke behavioural patterns due to the loss of neurons that have highly specific functions. As a matter of fact, in humans complete recovery of function in distal musculature is rare (Nudo et al., 1996). Thus, the performance improvement is partially due to compensation, which allows a partial return to pre-stroke motor performance levels.
As mentioned before, the motor and sensory cortices are organized in somatotopic functional maps showing high levels of use-dependent plasticity (Nudo et al., 1996). Motor maps reflect the coupling of specific neurons of the motor cortex to the muscles, while sensory maps represent the association of body parts to the neurons of the sensory cortex. Motor maps allow both the learning and the expression of movements and therefore represent a type of 'motor engram' or memory trace (Monfils et al., 2005). As a result, when the regions of the cortex are destroyed by a stroke, the motor engram is lost. As such, the only way to get a real recovery could be to replace the destroyed circuits, thus, the term recovery usually refers to various degrees of behavioural compensation that are provided by the remaining and newly developed brain circuits and that lead to altered behavioural patterns and/or tonovel strategies to improve performance.

1.3.2 Proportional recovery rule

The plasticity appears time-limited and has a peak in acute phase. In this time, the recovery is can be improved by rehabilitation therapy. This period of plasticity is related to spontaneous recovery which is observed in stroke patients. Recovery is variable and difficult to predict, i.e., only 38% of patients who showed an initially paralysed upper limb regained some dexterity by 6 months (Kwakkel et al. 2003), and in general two-thirds of patients perceived that loss of arm function was still a major problem after 4 years (Broeks et al. 1999).

Several factors are associated with poor outcomes, however the dominant one for predicting long term upper limb functionality is the initial severity of motor deficit (Coupar et al. 2012). The ability of initial deficit to predict upper limb recovery was first quantified such as “proportional recovery” rule (Prabhakaran et al. 2008). In line with theory, by 3 month, patients shall regain ~70% of its motor impairment showed on day 3 after stroke. In other words, the more severe is the deficit, the more the patient will recover, with a constant factor of 70%. However, initial deficit predicts outcomes only in patients with mild and moderate deficit. However, among patients who present high severity, recovery is proportional to the initial deficit in approximately half cases, in the other half case no substantial recovery is not seen **(Figure. 1.11)**. Indeed, it could be really interesting to understand if predictive factors exist, that could helping in distinguish in the early phase which patients will spontaneously recover later and which not.

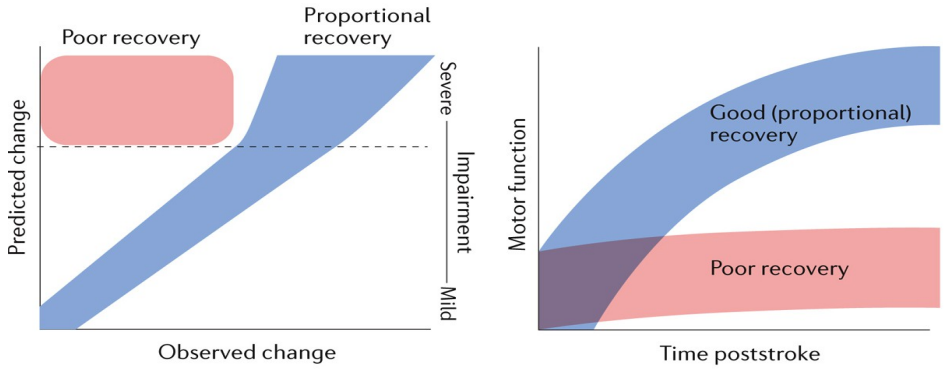

Figure1. 11: Different recovery curves of patients with initially severe upper limb impairment. *Recovery as predicted (blue) or poor recovery (red) (Ward 2017).*

1.3.3. Clinical outcomes

If an ischemic insult occurs in the motor cortex, one or more body parts contralateral to the infarct result impaired or paretic:~80% of stroke survivors experience impairment of movement on one side of the body (Langhorne et al, 2009). The degree of motor impairment depends on many factors, such as the extent of the infarct, the identity of the damaged region and the effectiveness of the initial neuroprotective interventions. In the first weeks after stroke, limited spontaneous recovery can occur. About 26% of stroke survivors are able to carry on everyday activities (Activity of Daily Living or ADLs, i.e. eating, drinking, walking, dressing, bathing, cooking, writing) without any help, but another 26% is forced to shelter in a nursing home (Carmichael, 2005). Impairments of upper and lower limbs are particularly disabling as they make very hard to have a sufficient degree of independence in ADLs.

Several scoring systems are exploited in the clinic to objectively quantify the impairment caused by a stroke. In human, the clinical quantification of impairments caused by a stroke is measured by two

main scoring systems. One of them is the National Institutes of Health Stroke Scale (NIHSS), composed of 11 items, each scoring a specific ability between a 0 and 4. For each item, a score of 0 typically indicates normal function in that specific ability, while a higher score is indicative of some level of impairment. The individual scores from each item are summed in order to calculate a patient's total NIHSS score. The maximum possible score is 42, with the minimum score being a 0. The NIHSS focuses on different aspects: level of consciousness, horizonal eye movements, visual field, facial palsy, movement of fore- and hindlimb, limb ataxia, somatosensation, language, speech and inattention. Another scale that is widely utilized in the field is the Fugl-Meyer Assessment, which is more specific for sensorymotor function. Each item of the scale is scored from 0 to 2: a zero score is given for the item if the subject cannot do the task and a score of 2 is given when the task is performed fully. However, reflex activity is measured using 2 points only, with a score of 0 or 1 for absence and presence of reflex respectively. Fugl-Meyer scale assesses five domains: motor function, sensory function, balance, range of motion of joints and joint pain. The maximum total score that can be obtained in Fugl-Meyer assessment is 226, though it is common practice to assess all domains separately.

1.4 Biomarkers of Stroke Recovery

1.4.1. Measures of motor function

Stroke remains a major cause of adult disability, and the recovery of motor function after stroke is crucial for the patient to regain independence. However, making accurate predictions of a patient's motor recovery and results is difficult if it is based only on clinical evaluation. Clinical assessment of motor impairment within a few days of stroke may help predict subsequent recovery, while neurophysiological biomarkers of corticomotor structure and function may help predict both motor recovery and motor outcome after stroke (Stinear, 2017). A biomarker of stroke recovery can be defined as an indicator of disease state that could be used to understand outcome or predict recovery or treatment response. In this context, it is useful to clarify the use of the terms “outcome” and “recovery”. “Outcome” refers to a measure at a single time-point, and is therefore insensitive to whether the patient’s motor performance has improved, remained stable, or deteriorated over time after stroke. In contrast, the “recovery” is evaluated over time and can be calculated as the absolute difference between baseline and subsequent clinical scores, or better as percentage of the available improvement in a specific scoring system.

The combination of biomarkers can provide clinically useful information when planning a patient's personalized rehabilitation. These biomarkers can also be used for patient selection and stratification in studies studying early post-stroke rehabilitation interventions. Ongoing multi-centre studies incorporating motor biomarkers could help bring their use into routine clinical practice.

A biomarker may also provide a measure of the underlying molecular/cellular processes, which may be difficult to assess directly in patients (Bernhardt et al. 2016). This would be particularly useful in identifying when and which neural mechanisms to target, and in some cases at what dose, with interventions to promote stroke recovery (Cramer et al. 2007). Methods for accurate long-term outcome/recovery prediction would allow clinical studies to be stratified on the basis of neurobiological recovery potential in a way that is currently not possible when studies are conducted in the absence of

valid biomarkers. Unpredictable results after stroke, particularly in those who do not follow the rule of proportional recovery (Krakauer et al. 2015), mean that clinical trials of rehabilitation interventions require hundreds of patients to be adequately fed. The use of biomarkers would allow to incorporate accurate information on the underlying damage, and therefore the size of these intervention studies could be greatly reduced, with obvious benefits (Winters et al. 2016). To be useful, a possible biomarker must explain the recovery beyond what is indicated by the initial damage, i.e. more than is currently achievable with the rule of proportional recovery. To fully understand the predictive capacity of biomarkers, it is necessary to conduct mechanistic studies, for which preclinical models are fundamental. In addition, conducting longitudinal studies would provide useful data to better predict the outcome or response of treatment.

Functional magnetic resonance imaging (fMRI) measures brain activity by detecting changes associated with blood flow. This technique is based on the fact that cerebral blood flow and neuronal activation are coupled: when an area of the brain is in use, the blood flow to that region also increases. This technique can also be used to study how the incidence of stroke affects brain function. The interaction between the affected cortex and its contralateral counterpart is a very interesting aspect in the field. A very useful fMRI parameter to address this point is the index of laterality of the primary motor cortex, i.e. how active the contralateral motor cortex is compared to the ipsilateral one during an unilateral motor task. In the subacute stage, the stroke condition is associated with a less lateralized activation than in healthy subjects, in particular an ipsilateral compensatory recruitment is observed (Feydy et al. 2002). An emerging notion in the field is that the greater the involvement of the affected motor network, the better the recovery. This hypothesis is supported by the increased activity of the primary motor cortex affected induced by motor training and acute pharmacological interventions, parallel to the improvement of motor function (Calautti et al. 2003). Dong and colleagues also demonstrated that the laterality index was able to predict response to constraint induced therapy (Dong et al. 2006). In addition to measuring the activity of precise brain areas during a particular task, fMRI allows the study of functional connectivity between different regions, examining the consistency of activation between them during rest. The results of functional connectivity of the resting state (rsFC) in the early and late subacute phases converge on the conclusion that interhemispheric connectivity is particularly important for motor control. Acute interruption of rsFC at the level of specific networks has been shown to be related to higher initial deficits (Carter et al. 2010, Baldassarre et al. 2016) and insufficient recovery at six months (Park et al. 2011).

Magnetoencephalography (MEG) or electroencephalography (EEG), non-invasive measures of cortical neuronal oscillations, are sensitive to alterations of cerebral blood flow (Nagata et al. 1989). In addition, multichannel recordings can provide insights on functional connectivity of brain areas, also in a spectral band-specific fashion. Several studies have focused on the correlation between spectral bands alteration and initial deficit. For instance, Wu et al. employed a regression analysis of spectral power with behavioural impairment scores (NIHSS), and established that higher delta power and reduced beta activity correlate with more severe NIHSS scores. More crucially, this relationship of high delta/low beta was prominent in electrode clusters overlying the ipsilesional sensorimotor cortex (Wu et al. 2016).

Apart from its usefulness for diagnosis, neurophysiological measurements have been shown to have some predictive power. The loss of power in the alpha band and the increase in the delta band

detected within 2 weeks of stroke are linked to an unfavourable outcome (Finnigan et al. 2013). In the same study, these indices were shown to provide unique, real-time information on the efficacy of thrombolytic therapy prior to clinical changes, thus informing decisions on alternative interventions (Finnigan et al. 2013). Consistently, Laaksonen and his collaborators found that patients with poorer stroke outcomes had persistent and increased low-frequency oscillations in acute and early and late subacute stages (Laaksonen et al. 2013), suggesting predominant inhibitory mechanisms in the peri-lesional cortex. Pushed to extremes, the absence of delta activity and the presence of theta and fast beta frequencies herald a benign course, here understood as patient survival (Burghaus et al. 2007).

As for fMRI studies, EEG allows to explore the connectivity between different brain area, looking at functional networks. Nicolo and collaborators recorded resting EEGs within 3 weeks of stroke symptom onset and coherence in the beta frequency band between the ipsilesional primary motor cortex and the rest of the cortex was evaluated. A higher coherence was correlated with improvements in a composite score of upper-limb motor performance during the first 3 months after stroke (Nicolo et al. 2015). In addition to resting state recording, EEG/MEG measurements can be performed also during the execution of a task. For instance, a movement-related desynchronization in the beta band at the level of primary motor cortex is observed when a subject produces an unimanual movement. When compared to control subjects, stroke patients exhibit a significantly reduced movement-related beta desynchronization (MRBD). Interestingly, within the patient group, smaller MRBD was seen in those with more motor impairment (Rossiter et al. 2014).

The translation potential of the EEG biomarker for patients is high, as the EEG is already part of standard clinical practice. However, further work is needed to develop automated data processing for easier use by physicians and to identify other EEG biomarkers that can make individual predictions rather than by patient groups.

1.4.2 Measures of anatomical/structural injury

Several structural biomarkers of neuroimaging have been studied in patients with stroke. These markers include quantitative characterization of the lesion of the stroke itself, as well as the structure and function of unharmed brain areas.

Acute infarct volume can be measured with computerized tomography (CT) or magnetic resonance imaging (MRI). Infarct size correlates with motor outcome, evaluated with the National Institute of Health Stroke Severity (NIHSS) score. However, this relationship is significantly attenuated with increasing leukoaraiosis (i.e. white matter disease) (Helenius et al. 2015). For what concerns the ischemic penumbra, recent data suggest that the site of ischemic penumbra, rather than volume, is the most informative parameter. As a matter of fact, infarction of an extremely well localized area of the periventricular white matter and the adjacent internal capsule is related to poor outcomes after MCA stroke (Rosso et al. 2014). Even the constriction of the damaged area can be an informative index, in fact, shrinkage of brain tissue was detected in all patients in the perilesional cortical structures (Kraemer et al., 2004). This study suggests that brain atrophy after acute ischemic stroke involved areas anatomically connected with the ischemic brain lesion but nevertheless was accompanied by a simultaneous improvement of the neurological deficit.

Another structure whose integrity is relevant for motor outcome is the corticospinal tract (CST). White

matter bundles integrity can be studied by means of diffusion-weighted magnetic resonance imaging (DW-MRI). This technique is based on the concept that water tends to diffuse more rapidly in the direction aligned with the internal structure that contains it, e.g. bundles of axons, and more slowly as it moves perpendicular to the preferred direction. Thus, it is possible to derive directional information of white matter tracts brain-wide. Measurement of CST integrity in the acute phase via diffusion tensor imaging (DTI, a modality of DW-MRI), which reflects fibre number, predicts motor recovery (Fugl-Meyer score) at 12 months. Another method use as biomarker the CST lesion load, calculated by overlaying the patient's lesion map on magnetic resonance imaging with a probabilistic CST constructed from healthy control subjects (Feng et al. 2015). Several studies have found that even when measured in the late subacute-chronic stage (> 4 months), the extent of CST injury also helps in predicting subsequent treatment response. For instance, Nouri and collaborators showed that those patients benefiting more from an epidural motor cortex stimulation had a smaller fraction of damaged CST compared to those who did not (44% vs 72%), and rarely had severe tract injury (Nouri et al. 2011).

However, an approach that integrates characteristics extracted from multiple brain areas, rather than only in the injured area, can better predict motor outcome and recovery. In a recent study, an automatic learning method was used to differentiate severe patients with subsequent good or poor recovery of the upper limb based exclusively on structural magnetic resonance imaging. The authors demonstrated that, while considering only CST damage led to a classification accuracy of 73%, the use of other motor areas (not the corticospinal tract) provided an accuracy of 87%, and the combination of both led to an accuracy of 90%. This proof of concept approach highlights the importance of considering different anatomical structures in order to better predict motor recovery (Rondina et al. 2017).

1.4.3 Combined approaches

The combination of neuroimaging and neurophysiological biomarkers can be useful in predicting motor outcomes and response to therapy. Limb outcomes above three months can be predicted in the first subacute phase by first measuring clinical biomarkers, then MRI in a stepwise approach, as established in the so-called PREP (Predicting Recovery Potential) algorithm (Stinear et al. 2012). As for the response to therapy, a recent study pointed out that the combination of neuroimaging structural damage characteristics and functional measures of the saved networks (e.g. EEG and fMRI) was the key to best predict the response to a standardized robotic therapy in the chronic phase (Burke Quinlan et al. 2015). The trials for rsFC, fMRI and MEG/EEG biomarkers are promising and represent a priority area of development.

1.5 Aims of the study

Stroke is a major cause of adult disability worldwide. Currently, there are no effective therapies to treat this condition and there valid methods to determine the extent of recovery in individual subjects. There is therefore a great need for reliable biomarkers that predict spontaneous recovery and new approaches to stimulate the recovery of lost functions.

In this study I exploited a mouse model of stroke, the Middle Cerebral Artery Occlusion (MCAO), that showed a high variability in outcome and it is thus close to the human condition. I conducted experiments to evaluate the occurrence of motor deficits using different behavioural tasks: gridwalk test, skilled reaching test, and retraction task in the M-platform (a robotic device that permits to quantitatively evaluate several kinetic/kinematic parameters related to forelimb movement). Moreover, the ischemic lesion and electrophysiological alterations were analysed by means of histology and electroencephalographic signals respectively. I studied how these parameters were altered by stroke. Finally, I combined behavioural and anatomical data in order to define possible biomarkers that predict long-term motor recovery.

Chapter 2. Materials and Methods

2.1 Experimental design

All procedures have been performed according to the guidelines of the Italian Ministry of Health for the care and maintenance of laboratory animals, and in strict compliance with EU Directive No 2010/63/EU on the protection of animals used for scientific purposes. Animal testing at the Institute of Neuroscience of the CNR has been approved by the Italian Ministry of Health. All surgical interventions were performed under deep anaesthesia and all efforts were made to minimize animal suffering. To study the physiological changes that occur during MCAO induction, a total of 38 C57BL6J mice (weighing 20-28g, age 8-12 weeks) were used.

Firstly, animals were trained to learn the skilled reaching task for two weeks. Then, animals underwent electrode implant and trained for an additional week in order to allow them to re-habituate to the skilled reaching task after the surgery. During this re-habituation period animals were also shaped on the robotic platform. At the end of the week the baseline performance in the skilled reaching, gridwalk test and on the M-platform was acquired. MCAO was induced in the right hemisphere. Finally, animals underwent behavioural testing in the gridwalk, skilled reaching test, M-platform at day 2 and 30 post MCAO.

Moreover, to investigate possible post-stroke changes, the animals were recorded electrophysiological both in freely-moving condition and during a retraction task on a robotic platform once every two weeks **(Figure 2.1)**. After 30 days, in order to perform anatomical analysis, animals were intracardially perfused and immunohistochemistry assay was performed.

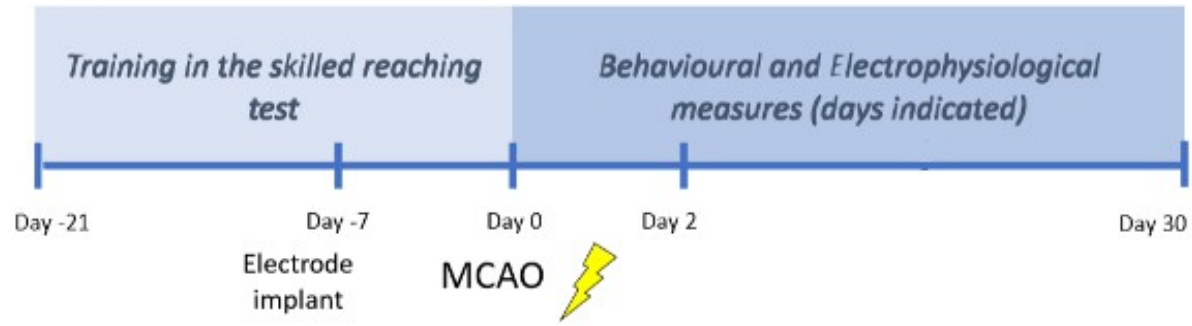

Figure2. 1: Timeline of experiments

2.2 Electrode Implant

Animals were anesthetized with avertin (20ml/kg, 2,2,2 tribromoethanol 1.25%; Sigma-Aldrich, USA), placed in a stereotaxic apparatus and the skull was exposed through a midline incision. Then, two burr holes were drilled in both hemispheres at the level of Bregma (zero coordinate), 2mm lateral **(Figure. 2.2)**.

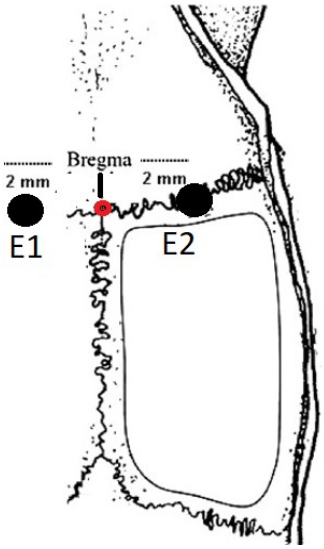

Figure2. 2: Location of EEG electrodes. *E: electrode covering motor cortex*

This way, the electrodes were implanted in the caudal forelimb area (CFA) (Tennant et al 2001, Alia et al. 2016). A surgical screw was tightened at the centre of the occipital bone and was used as ground reference. Bipolar electrodes were assembled prior to the surgery: a couple of twitched insulated tungsten wires (700µm spaced in length at the tip) were soldered at the channel and reference pins of the connector (Elitalia). After screw positioning, the electrodes were stereotactically inserted in the centre of the drilled holes, at a depth in which the shorter wire was in contact with the dura mater, and the ground pin was connected to the occipital screw. A first layer of dental cement (Optibond) was distributed to secure all the components to the skull surface. After the first layer of cement was dried, an aluminium post, used later to head-fix the animal, was cemented onto the skull. Finally, a second layer of cement (Paladur, Pala, Germany) was distributed to enclose all the electrical components. After the surgical procedure, animals were treated with paracetamol (100mg/kg) for 4 days post-operation in drinking water.

2.3 Permanent Middle Cerebral Artery Occlusion

Animals were anaesthetized with avertin (20ml/kg, 2,2,2 tribromoethanol 1.25%; Sigma-Aldrich, USA), transferred onto a heat blanket in lateral position and immobilised with adhesive tape for medical use. A skin incision was performed between the ear and eye using surgical scissors. Then, the temporal muscle was exposed, detached from the bone and cut vertically to show the underlying skull. The MCA was identified and a craniotomy was drilled above it. Once it was exposed, the MCA was occluded with electrocoagulation forceps (biological instruments, bipolar mode, 12W). If spontaneous recanalization occurred, the electrocoagulation was performed again. Finally, the temporal muscle was relocated to its position, glued and the wound was sutured. Sham animals underwent the same procedure but without the electrocoagulation step. After the surgical procedure, animals were treated with paracetamol (100mg/kg) for 4 days post-operation in drinking water.

2.4 Immunohistochemistry

Brains were collected after transcardial perfusion of deeply anaesthetized mice with PBS (5 min) followed by 4% PFA. Brains were then post-fixed in 4% PFA for 2 hours and then kept in 30% sucrose in Phosphate Buffer at 4°C. Then, they were sectioned on a sliding microtome (Leica, Germany) into 50µm thick coronal sections, which were kept free-floating for further processing. Brain slices were incubated in a blocking solution for 1 hour (10% horse serum; 0,3% Triton X-100 in PBS) before applying the primary antibodies, dissolved at the proper concentration in 1% horse serum and 0.2% Triton X-100 in PBS. The following primary antibodies were used: guinea pig a-NeuN (1:1.000, Millipore), rabbit a-GFAP (1:500, Dako). After washing, slices were incubated with species-specific secondary antibodies, dissolved in 1% horse serum and 0.2% Triton X-100 in PBS, for 2h at room temperature. Nuclear staining was performed with (1:500) Hoechst (33342 Sigma). Coverslips were mounted on glass slides with Vectashield. Images were acquired with epifluorescence microscope equipped with Apotome (Zeiss).

2.5 Anatomical/structural measures

2.5.1 Lesion volume and CFA integrity

The volume and location of the lesion were assessed. In addition the enterity of the CFA, and the shrinkage of the perilesional cortex were measured using an innovative overlapping-masks system **(Figure 2.3)**.

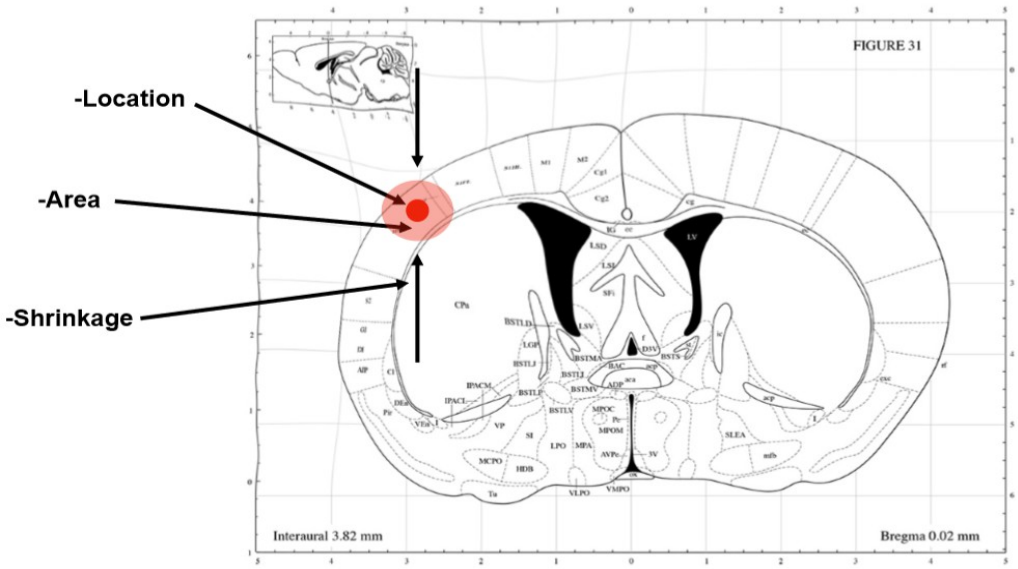

Figure2. 3: Measures considered after stroke

For anatomical analyses 1 out of every 6 sections was stained with NeuN and GFAP. The lesion volume and the volume of the affected CFA for each animal were calculated by summing up all damaged areas and multiplying the number by section thickness and by 6 (the spacing factor). To avoid an underestimation of the lesioned volume due to the brain shrinkage that take place in the ipsilesional cortex after the stroke, each damaged areas in each single brain slice was normalized by its cortical shrinkage before summation (see below for the calculation of the cortical shrinkage) as

follow:

$$Normalized\ Area\ of\ the\ Lesion = \frac{Measured\ Area\ of\ the\ lesion}{1 - Cortical\ Shrinkage}$$

To quantify the integrity of the CFA, we took advantage of previous findings on motor cortex mapping. A red area, responsible for a forelimb movement in the 100% of tested animals and a yellow area, responsible for a forelimb movement in the 50% of tested animals were identified and superimposed on each coronal section mask **(Figure 2.4)**. Then, each mask was overlapper and adapted to the corresponding histological brain slice for the entire extension of the CFA, (from approximately -1,00mm posterior up to +1,25 anterior to Bregma 0 suture). The adaptation of the masks to the histological brain slices was accomplished using Photoshop filters. Subsequently, using a digital elaboration software (ImageJ), the lesion contour was drawn, thus lesion area and the percentage of CFA affected were measured.

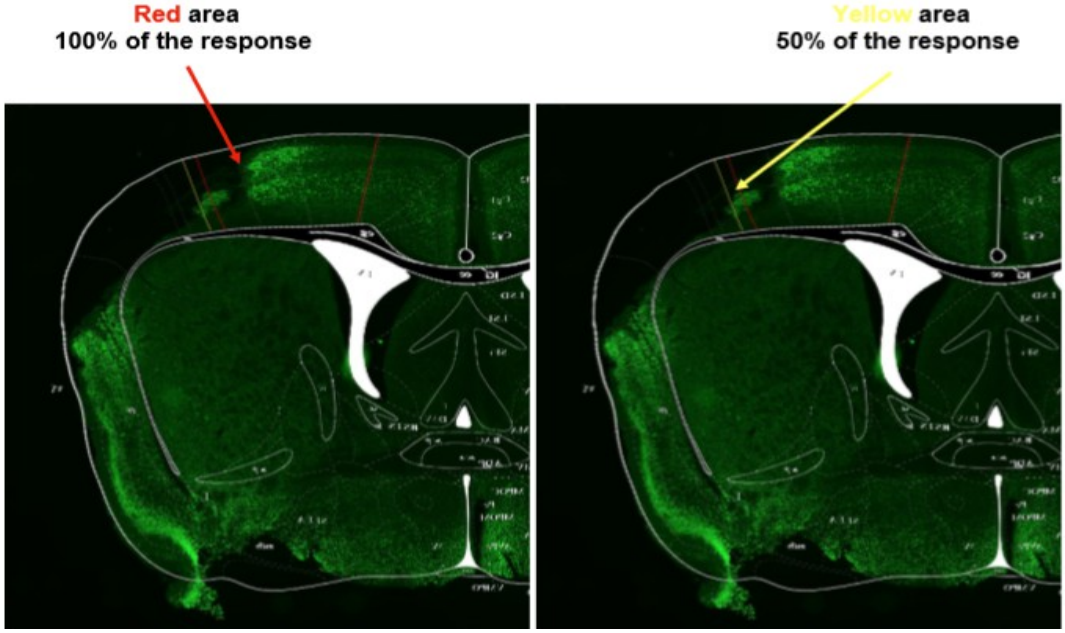

Figure2. 4: Lesioned CFA

The shrinkage of the tissue was measured firstly computing a volumetric factor (Vf), i.e. the ratio between the healthy contralateral cortex and the corresponding section on the Paxinos atlas, thus accounting for the real dimension of each brain. Then, the atlas cortical area for each section has been multiplied by the Vf to obtain the ideal cortical dimension of each section. Then the ipsilesional cortical area was measured for each slice. Then we calculated the % of Cortical shrinkage (Cs) as the difference between the theoretical and real cortical areas normalized on the theoretical one and multiplied by 100 **(Figure 2.5)**. Finally lesioned area for each section was divided by (1-Cs) and then translated in a volumetric measure by summing up all corrected lesioned areas and multiplying the number by section thickness and by 6 (the spacing factor).

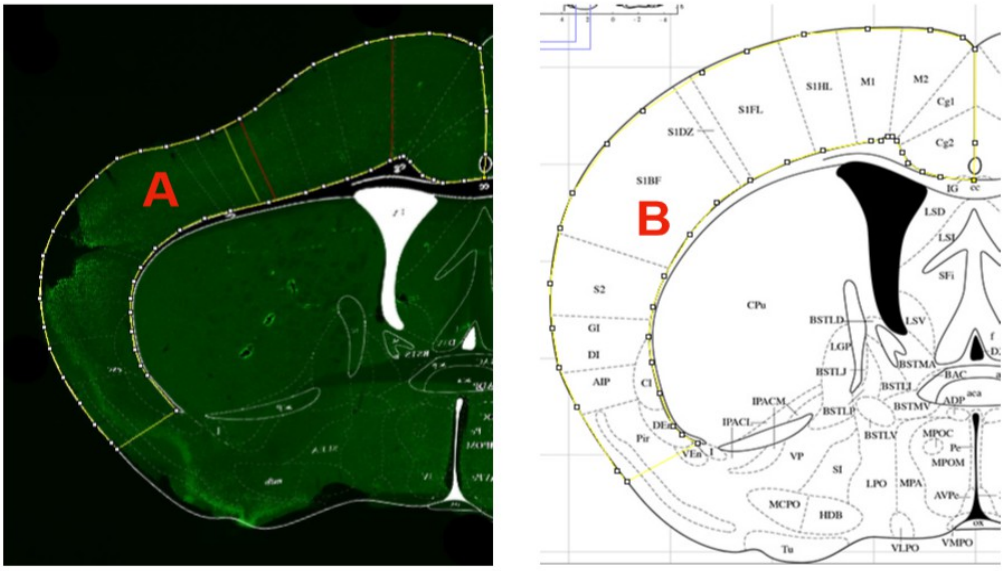

$$\% \text{ Shrinkage} = \left(\frac{B - A}{B}\right)100$$

Figure2. 5: Example of shrinkage and distortion.

2.5.2 White matter integrity

In order to test the hypothesis that loss in the descending motor pathways, measured at the level of internal and external capsule, would determine motor deficit after a cortical stroke, the integrity of the white matter was measured using a Luxol fast blue staining **(Figure 2.6)**.

For each animal 2 50um-thick coronal brain slices located at 0mm, 0,5 mm and 1mm posterior to Bregma 0 were chosen. These slices were mounted on a gelatin-coated slide, then were rehydrated in distillate water for 1 minute, ethanol 50%, ethanol 70%, ethanol 96% for 3 minutes each, so, slides were incubated at 60°C with a Luxol fast blue solution overnight. Then slices were left to cool, after that they were placed in ethanol 96% 2 minutes for 2 times, ethanol 70% and ethanol 50% for 3 minutes each. Distillate water 3 minutes for 2 times, lithium carbonate for 10 minutes, distillate water 3 minutes for 2 times, periodic acid for 8 minutes, distillate water 3 minutes for 2 times and sulfur dioxide solution 1 minute for 3 times. Slices were rinsed in running water for 15 minutes, than they were dehydrated in ethanol 50%, ethanol 70%, ethanol 96%, ethanol 100% for 3 minutes each and xylene for 5 minutes. Slices were mounted with DPX. Successively, slices were acquired using 20x magnification. Finally we measured ipsilesional and contralesional area of the internal and external capsula using the elaboration software ImageJ.

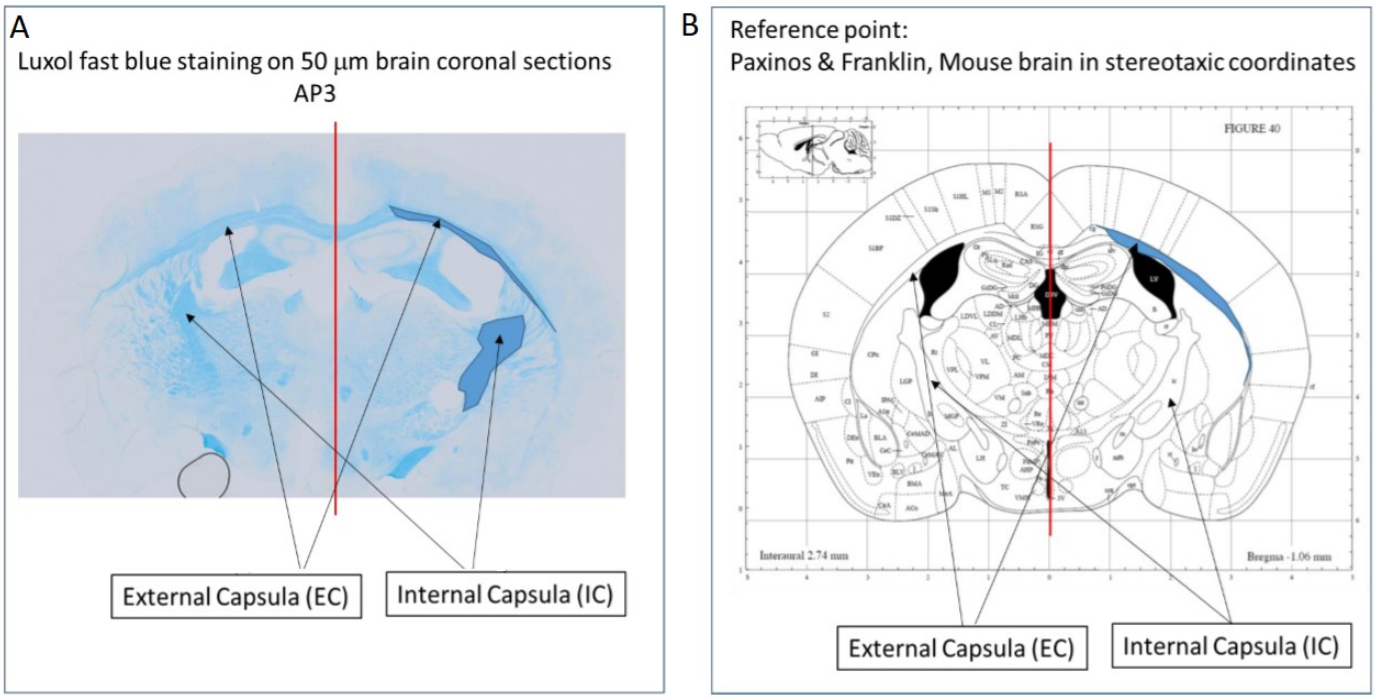

Figure2. 6: White matter assessment. (A) *Internal and Eternal capsule of -1,00 Bregma slices were labelled using Luxol fast blue staining.* ***(B)*** *Mouse brain atlas used as a reference.*

2.6 Behavioural tests

2.6.1 Reaching test

The animals (food deprived for 15h) were placed in a testing chamber with plastic walls (0.5x1.3cm) and trained to perform a skilled reaching test with their preferred paw, which had to pass through a small frontal rectangular aperture to grasp and retrieve food pellets **(Figure. 2.7 A)**. The task was video recorded from the side of the tested forelimb. Each attempt was classified as follows: (i) correct: the pellet was grasped and taken directly to the mouth; (ii) dropped: the pellet was grasped but it fell right before entering the chamber or inside of it; (iii) displaced: the pellet was not grasped but just displaced from its position; (iv) missed: the paw crossed the frontal window but the pellet was not displaced.

Then, the percentage for the single categories was calculated over the total attempts, a cumulative score of the performance was calculated as follows:

$$ReachingScore = \%Correct + 0.66 \cdot \%Dropped + 0.33 \cdot \%Displaced + 0 \cdot \%Missed$$

2.6.2 Gridwalk test

Animals were allowed to freely walk for 5 minutes on an elevated grid (32x20cm, with 11x11mm large openings) and the task was video recorded **(Figure. 2.7 B)**. The video recordings were analysed off-line by means of a custom-designed Graphical User Interface implemented in Matlab, to assess correct steps and foot-faults, i.e. steps not providing body support, with the foot falling into grid hole. The percentage of foot faults for each limb was then calculated.

$$FootFaults\% = 100 \cdot \frac{\#foot\ faults}{\#corret\ steps + \#foot\ faults}$$

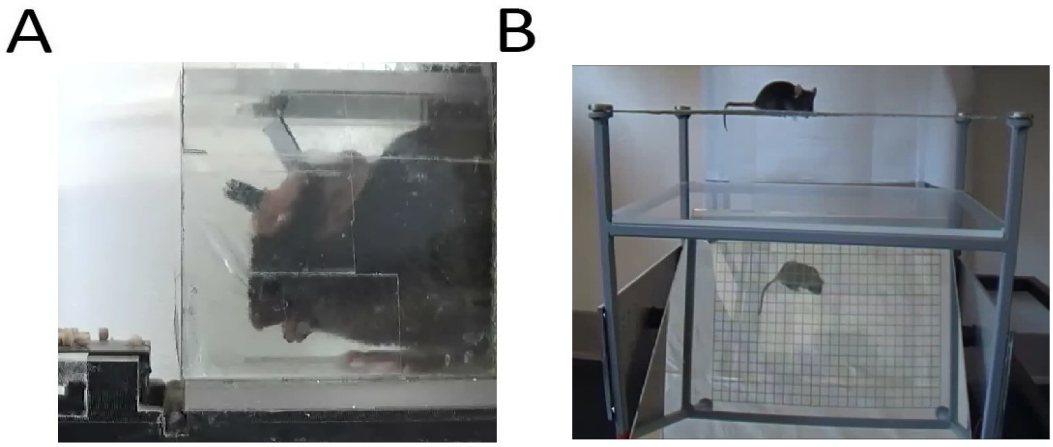

Figure2. 7: Behavioral tests. (A) *Reaching task.* ***(B)*** *Gridwalk test.*

2.6.3 Robot task

We measured forelimb performances in a robotic device, the M-Platform **(Figure. 2.8)**, where the animal had to pull back a handle in order to get a liquid reward (Spalletti et al., 2014, 2017) thereby allowing the assessment of kinetic and kinematic parameters.

The main components of the M-platform **(Figure. 2.8 A)**, are a linear actuator (Micro Cylinder RCL, IAI, Germany), a 6-axis load cell (Nano 17, ATI Industrial Automation, USA) and a custom designed handle that was fastened to the wrist of the mouse and placed on a precision linear IKO slide (IKO BWU 25-75, USA).

During experiments, the animal was kept in a U-shaped restrainer (interior dimensions 35×80×30mm) and head-fixed on the platform by means of a post cemented to the skull. Its left wrist was blocked to the slide through the handle.

The task was a pulling/retraction movement and included two phases: a passive phase and an active phase. During the first phase the linear actuator pushed the slide, where the wrist of the animal was blocked, to extend its forelimb in parallel to the sagittal plane. Then, the active phase started and the motor was quickly decoupled from the slide and the animal could voluntarily pull back the slide to the rest position. Animals were water-deprived for 15h and receive a milk droplet as a reward for each complete retraction.

Several robot parameters were evaluated: (i) the latency to the first retraction (i.e. the time elapsed before the first force peak) (ii) the t-target, i.e., the time spent by the animal to accomplish a single retraction task; (iii) the number of sub-movements needed to complete the task; (iv) the number of attempts, i.e., the number of force-peaks not corresponding to a sub-movements (i.e. below the static friction force) **(Figure. 2.8 B)**. For each session, a number of 25-30 trials, i.e. full extension-retraction cycles, were performed.

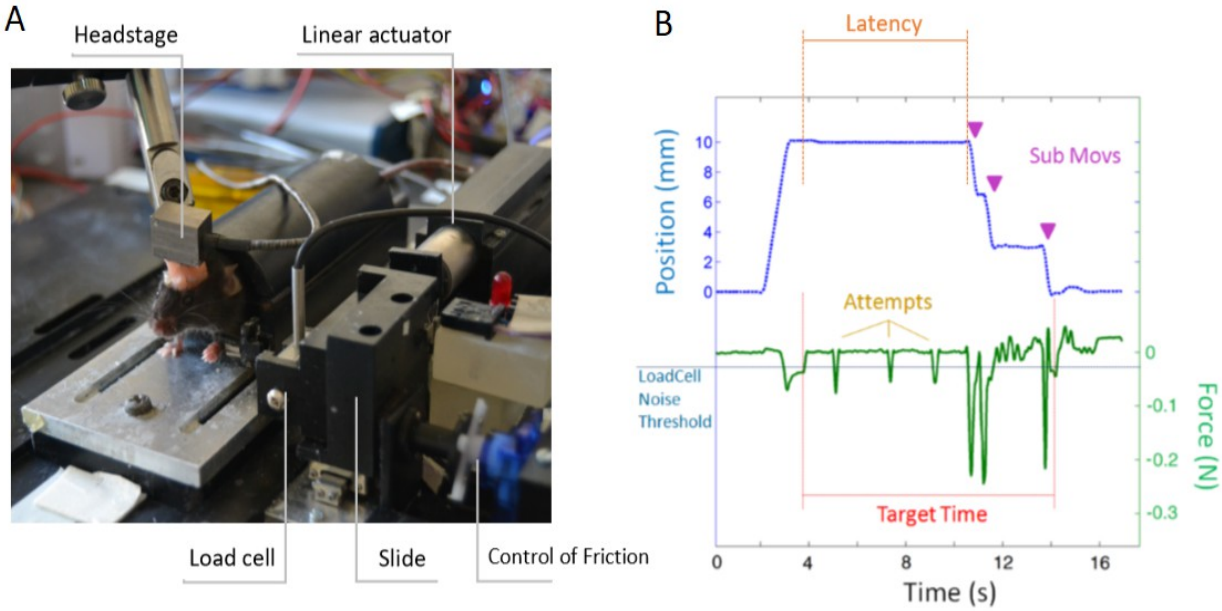

Figure2. 8: M-Platform. *(**A**) Main components of the M-platform. (**B**) Parameters extracted from retraction movement.*

2.6.4 Motor score

In order to combine all behavioural informations, we implemented a global motor score, that contain all behavioural tests in a single total score. For this, the scores of each behavioural tests are converted in a scale from 0 to 10. Score 0 was assigned to animals that didn't have a good performance, while score 10 to extremely high performing animals.

For each test the score was assigned as follow:

- **Gridwalk test:**

  10%-60% errors → 10-0 score

  < 10% errors → 10 score

  > 60% errors → 0 score

- **Reaching test**:

The entire dynamic range was maintained.

- **Robot task:**

  Latency 0-1000 → 10-0 score

  >1000 → 0 score

  T-target 0-2500 → 10-0 score

  >2500 → 0 score

Attempts	0-5 → 10-0 score
	>5 → 0 score

The same classification was applied for the isometric measures.

Amplitude	0-0,8 → 0-10 score
	>0,8 → 10 score
AUC	0-15 → 0-10 score
	>15 → 10 score

2.6.5 Statistical Analysis

All statistical tests were performed using SigmaPlot 12.0 (Systat Software Inc, USA). For comparisons between different groups, a Two-Way Repeated Measures ANOVA was used followed by Tukey Test. In all graphs, data are reported as mean ± standard error.

2.7 Neurophysiological recordings

2.7.1 Electrophysiology in freely moving

Spontaneous neuronal activity in both controls and ischemic animals was acquired during freely moving behaviour before surgery and then once every two weeks, starting from day 2. Recordings were performed in a test cage for a 30min session, using a 2channels extracellular amplifier (Npi electronic, Germany). Cortical local field potentials (LFP) were 10’000X amplified and 0.3–100Hz band-passed. We focused on estimating the power content of the standard neurophysiological spectral bands: delta = (0.5 − 4) Hz, theta = (4.1 − 8) Hz, alpha = (8.1 − 12) Hz, beta = (12.1 −30) Hz, gamma = (30.1−50) Hz of the LFP signal.

2.7.2 Electrophysiology onto the robotic platform

Recordings of local field potentials (LFPs) were performed from both hemispheres during the retraction task in the M-Platform. Signals has been bandpass filtered (3 - 100Hz), amplified and fed to recording system (Plexon). Recordings were carried out before and at 2 and 30 days after MCAO. From these recordings, we estimate several physiological parameters, including the distribution of LFP power in the different spectral bands, amplitude and latency of event-related potentials (ERPs) triggered by force peaks measured in the M-Platform.

Data were processed with the software NeuroExplorer to obtain the the event-related potentials (ERPs) associated with the force peak generation. Neural signals were aligned on the onset of the force peak and amplitude parameter were extracted by means of a Matlab custom-made GUI.

Chapter 3. Results

3.1 Post-stroke anatomical alterations

3.1.1 Lesion volume and cortical integrity

Permanent Middle Cerebral Artery Occlusion (MCAO) is an experimental model close to the human condition, in which a significant percentage of strokes affects the territory of the MCA. To understand if this model could represent the human condition also in terms of variability of the lesion volume, allowing us to investigate mechanisms that go beyond spontaneous motor recovery, we have characterized anatomical changes that occur 30 days after the stroke. Thus, we assessed the lesion volume in the targeted cortical areas and via immunohistochemistry for a neuronal and an astroglial marker, i.e. NeuN and GFAP respectively **(Figure 3.1)**. At 30dpl, within the lesion, the NeuN signal could still be detected, but its pattern was extremely different from that of the healthy cortex **(Figure 3.1 A-C)**: in fact, after the lesion neurons appeared narrower and less dense **(Figure 3.1 D, E)**. Intense astrogliosis was present in a large portion of the ipsilesional hemisphere, particularly along the contour of the lesion **(Figure 3.1 F)**.

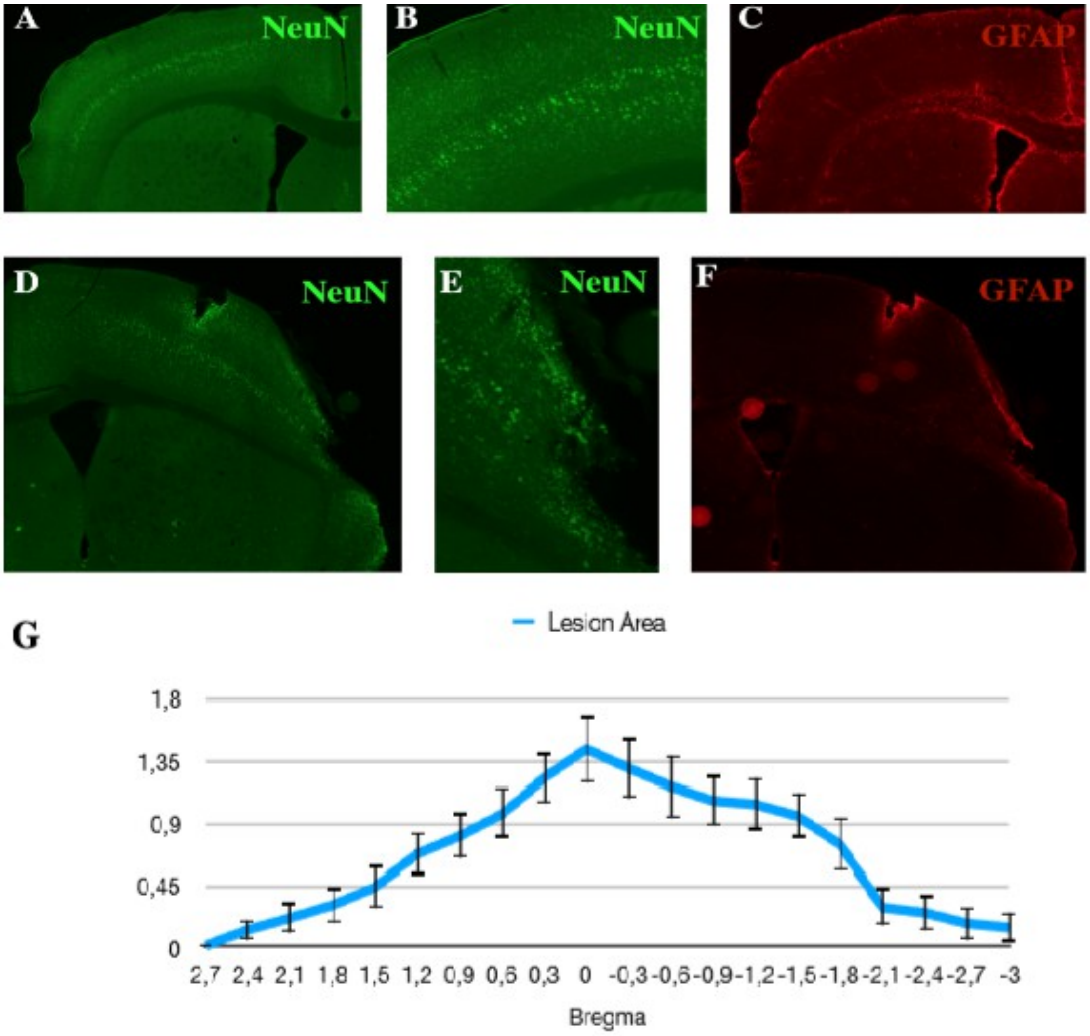

Figure3. 1: Histological brain slices at 30dpl. ***(A)*** *NeuN staining of histological brain slice at bregma level of* healthy cortex*.* ***(B)*** *Detail of the sane cortical thickness that show its typical pattern.* ***(C)*** *GFAP staining of histological brain slice of* healthy cortex *at bregma level.* ***(D)*** *NeuN immunoistochemistry of histological brai slice 30 days after MCAO induction.* ***(E)*** *Detail of the lesion.* ***(F)*** *GFAP immunoistochemistry of histological brain slice 30 days after MCAO induction.* ***(G)*** *Representation of lesion extension at 30dpl along the anteroposterior axis (n=15). In the x axis Bregma level, in the y axis lesion volume.*

Among the animals (n=15), the lesion had a volume of 4.00 ± 0.625 mm3**,** covered a region between 2.4 mm anterior to Bregma 0 and 2.1 mm posterior to Bregma 0, and reached its maximum area around the Bregma 0 suture **(Figure 3.1 G)**. We found a considerable variability in terms of localization of the lesion along the mediolateral axis. This high variability in the location of the lesion can be easily appreciated by comparing the same cerebral coronal slice of different animals undergoing MCAO **(Figure 3.2)**.

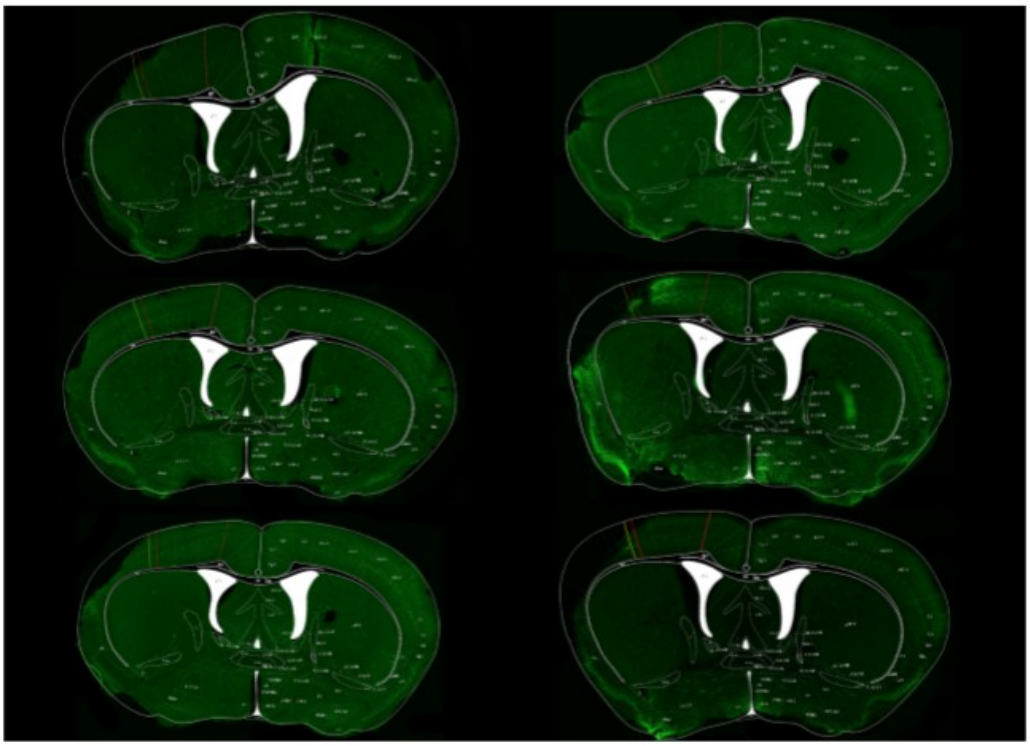

Figure3. 2: NeuN staining of at Bregma level 0 in six different MCAO animals 30dpl. *The same mask was superimposed on each slice to highlight Caudal Forelimb Area location.*

The distortion caused by shrinkage is an important parameter that could contribute to neural impairment due to tissue compression, so it could be considered as a possible biomarker. On average, the lesion reduced the ipsilesional cortical area by 19.36 ± 2.25 %, and neural tissue contraction tended to be greater around Bregma 0 where the area of cortical damage is larger **(Figure 3.3 A)**. As expected, the percentage of ipsicortical shrinkage among animals strongly and positively correlates with the extension of the lesion volume. In fact, after a stroke, the ischaemic area fills rapidly with scar tissue, which, after the reduction of the initial oedema, tends to shrink, leading to the lengthening of the perilesional tissues and an eventual worsening of the initial damage **(Figure 3.3 B)**.

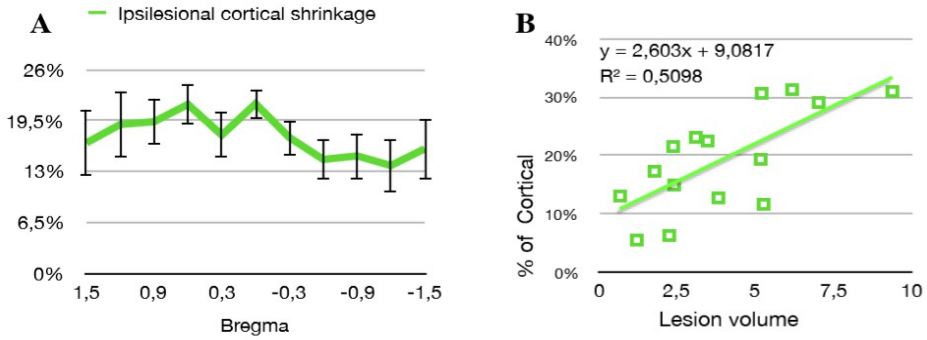

Figure3. 3: Ipsilesional cortical shrinkage at 30dpl. (A) *Percentage of ipsilesional cortex shrinkage along the anteroposterior axis. In the x axis Bregma level, in the y axis percentage of shrinkage in the lesioned hemisphere.* ***(B)*** *Correlation among cortical shrinkage and lesion volume (linear regression R=0,713989) (n=15). In the x axis lesion volume, in the y axis percentage of shrinkage in the lesioned hemisphere.*

The ischaemic lesion mainly interested the somatosensory areas, while motor areas, including the CFA, were only partially affected. A damage in the CFA should directly affect the motor performance of the contralateral forelimb. However, previous studies highlight the great potential of perilesional tissues to partially guide the recovery of lost motor function through neuroplastic rearrangements of the surrounding motor cortex (Alia et al. 2016). Out of the 15 MCAO animals, only 5 showed significant ischemic damage in the CFA (percentage of injured CFA > 5%) **(Figure 3.4 A)**. The same five animals also had the largest lesions, with the somatosensory area as the main target of the MCAO, while the CFA resided in the perilesional site and was involved only with larger lesions. Among these animals (n=5) 12.86% ± 1.95% of the CFA was injured, with greater posterior damage to the Bregma 0 suture **(Figure 3.4 B)**.

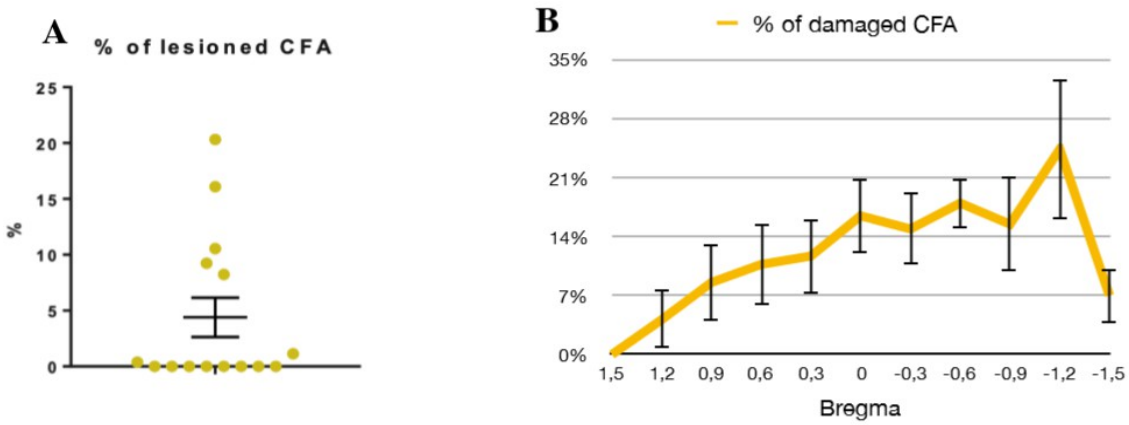

Figure3. 4: CFA lesion on 30dpl histological brain slice. (A) *Percentage of lesioned CFA among MCAO mice (n=15).* ***(B)*** *Percentage of damaged CFA along anteroposterior axis in animals that reported a consistent (>5%) damage in CFA (n=5). In the x axis Bregma level 0, in the y axis percentage of CFA damaged.*

3.1.2 White matter integrity

Today, the most robust imaging biomarkers to predict motor recovery and outcome in humans after stroke are measures of white matter integrity of the corticospinal tract (CST). To study this aspect on the murine MCAO model, we directly measured the integrity of the white matter in the internal and external capsule on histological slices of the brain obtained 30 days after the induction of the lesion. The white matter was stained with Luxol fast blue and measurements were performed on slices of 0mm, 0,5mm and 1mm behind the Bregma 0 (see Materials and Methods) **(Figure 3.5)**.

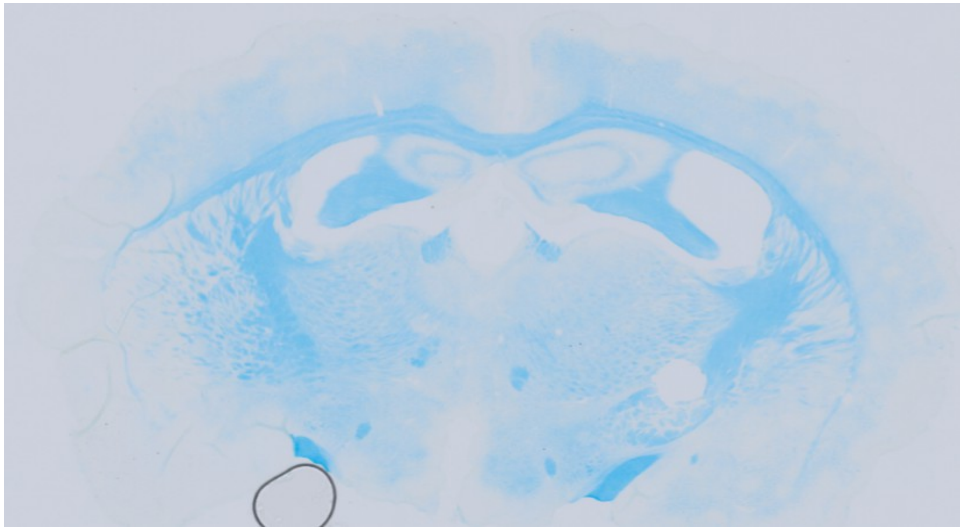

Figure3. 5: Histological brain slice stained with Luxol fast blue protocol. *Example of sane brain coronal sections of 1mm behind the Bregma 0.*

We found that the ratio between ipsilesional and contralesional quantities of white matter was lower for the MCAO animal than for Sham, measuring both the external (n=17) and internal (n=8) capsules. However, only the difference in the external capsule area was statistically relevant when compared between sham and MCAO animals ($p < 0.05$). It is possible that the differences related to the internal capsule were not statistically significant because of the lower number of animals analysed **(Figure 3.6)**.

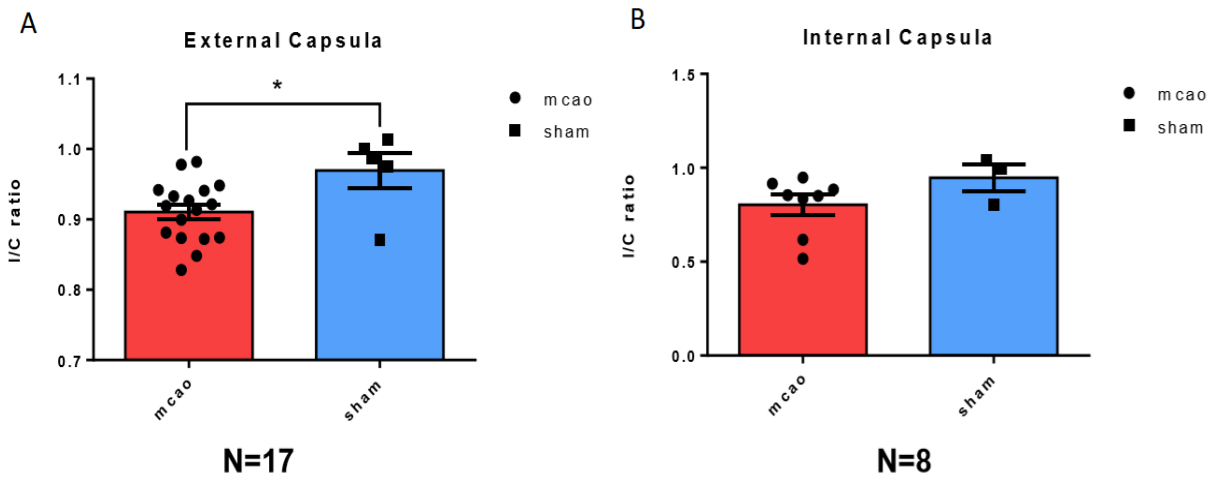

Figure3. 6: Ipsi/Contra ratio of white matter integrity. (A) *Ipsi/contra ratio integrity of the External Capsula.* ***(B)*** *Ipsi/contra ratio integrity of the Internal Capsula. *' represents significant difference from the baseline: *, $p < 0.05$.*

3.2 Alterations in motor function after MCAO

In order to evaluate the deficit at the behavioural level we exploited different motor tests evaluating the general functionality or fine motor control. One of these test is the skilled reaching test, which allows to evaluate finer motor performance, i.e. the grasping of a food pellet. After 2-3 weeks of training, baseline performance was measured and then the test was repeated at 2dpl (acute phase) and 30dpl (chronic phase). During the scoring procedure, "correct" movements and errors were evaluated. In addition, errors were further divided into "dropped", "displaced" and "missed" (see Materials and Methods). As expected, after the lesion, we observed a significantly decrease in the number of "correct" movements at 2dpl in MCAO group (n=25), whereas the sham group did not show significant differences ($p<0.001$) **(Figure 3.7 A)**. At the behavioural level, we observed that lesioned animals started to generate "clumsy movements", in which the animal is not able to grasp the pellet or even to centre the frontal aperture and that were thus classified as "missed". We reasoned that this "missed" category represented the most severe type of error, given that in this case the animal is not even able to reach or displace the pellet, in fact percentage of errors, in particular missed movements increased after stroke **(Figure 3.7 B)**. The sham group did not show significant differences (n=13).
Given that motor performance in the skilled reaching test appeared quite variable even for the same animal, we exploited a cumulative score in which a fixed value is attributed to each class of movements: 1 for "correct", 0.66 for "dropped", 0.33 for "displaced" and 0 for "missed". This scoring method revealed to be more robust than just considering the number of "correct". We observed a functional decrease at 2dpl with a spontaneous recovery at 30dpl **(Figure 3.7 C)**.

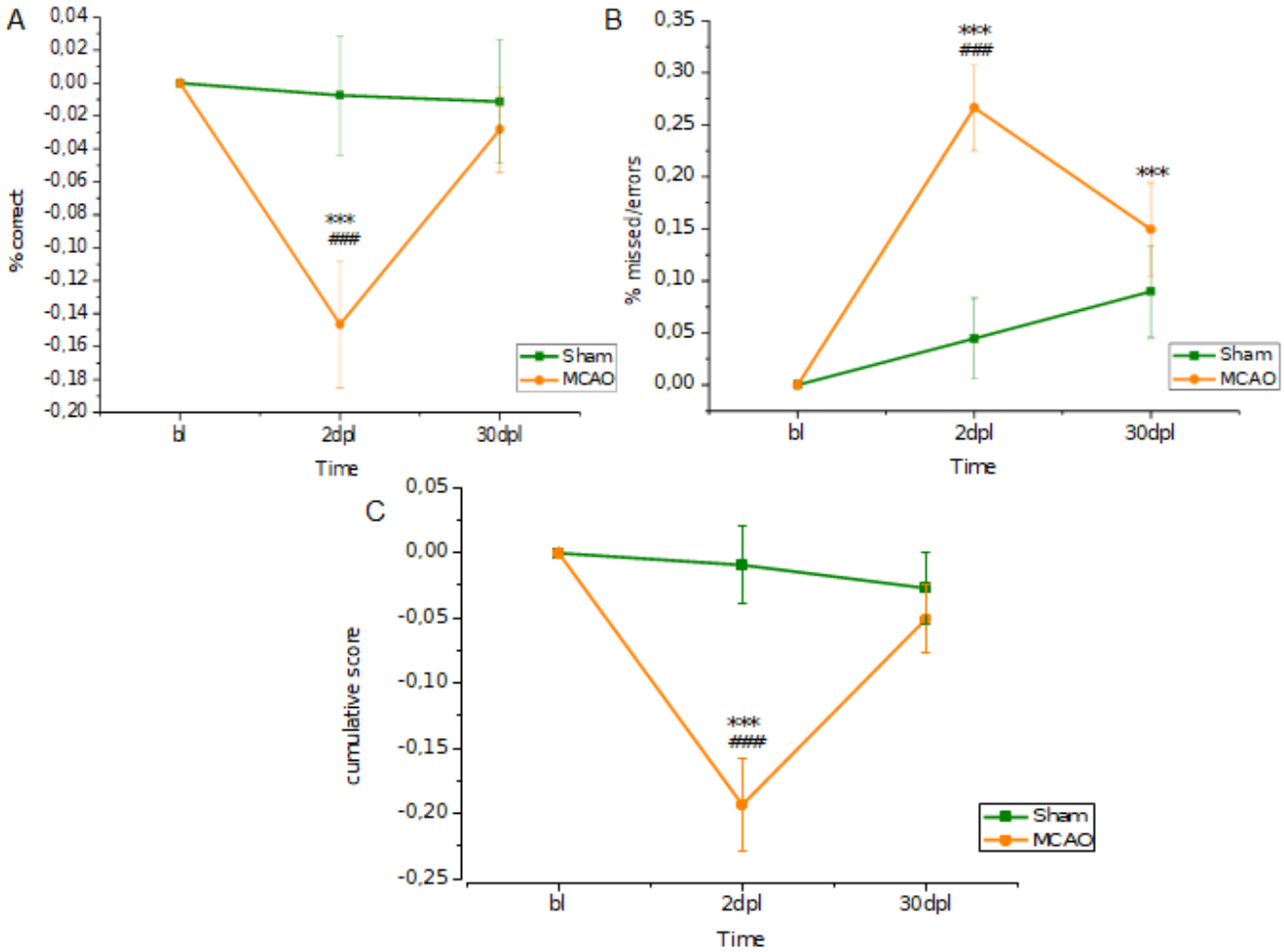

Figure3. 7: Analysis of skilled reaching test performance. (A) *Percentage of "correct" before and after MCAO induction.* ***(B)*** *Proportion of "missed" over the total number of "errors".* ***(C)*** *Cumulative score. (*) represents significant difference from the baseline, ***, p < 0.001. '#' represents significant difference from the sham group, ###, p < 0.001. (n=38; MCAO=25, sham=13).*

An easy way to assess motor damage of all the four limbs is the gridwalk test. An animal is placed on an elevated grid with opening (see Materials and Methods). Animals without brain damage usually put their paws precisely on the wire frame to hold themselves while moving along the grid. Each time a paw slips through an open grid, a "foot fault" is recorded. Sham animals generally show few foot faults for both forelimbs. We evaluated the percentage of foot faults in both the affected (i.e. contralateral to the lesion) and healthy (i.e. ipsilateral) forelimb. After the induction of MCAO, there was a significant deficit in the use of the affected forelimb at 2dpl ($p<0.001$), which did not recover up to 30dpl. We observed a significant difference with the sham group for both time points considered ($p<0.001$, MCAO=18, sham=13) **(Figure 3.8)**.

Moreover, we used a robotic platform developed in our lab, the M-platform, to add a quantitative measure of the motor deficit induced by the MCAO. This device provides a quantitative assessment of anterior limb flexion movement, is sensitive to detect performance deficits after a localized cortical stroke, and measures functional improvements during post-stroke training (Spalletti et al. 2014, Pasquini et al. 2018). Mice (n=29) were allowed to familiarize with the setup for a week before measuring baseline performance and then, animals were tested again on the robotic platform at

2 and 30 days after the injury. We analysed 4 different parameters: latency, t-target, submovements and attempts **(Figure 3.9)** (see Materials and Methods).

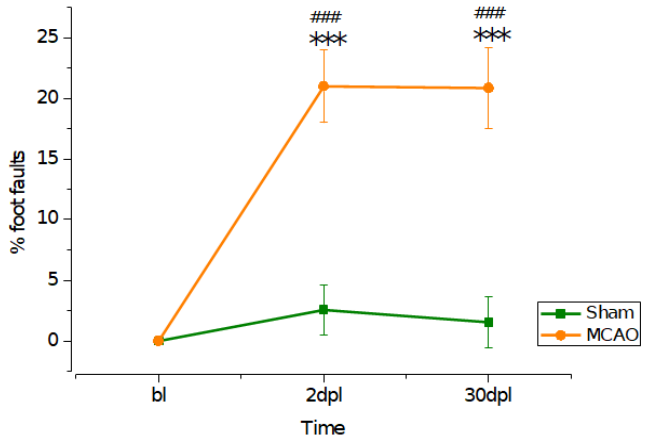

Figure3. 8: Analysis of gridwalk test performance. *Percentage of foot faults. (*) represents significant difference from the baseline, ***, p < 0.001. '#' represents significant difference from the sham group, ###, p < 0.001 (n=31; MCAO= 18, sham=13).*

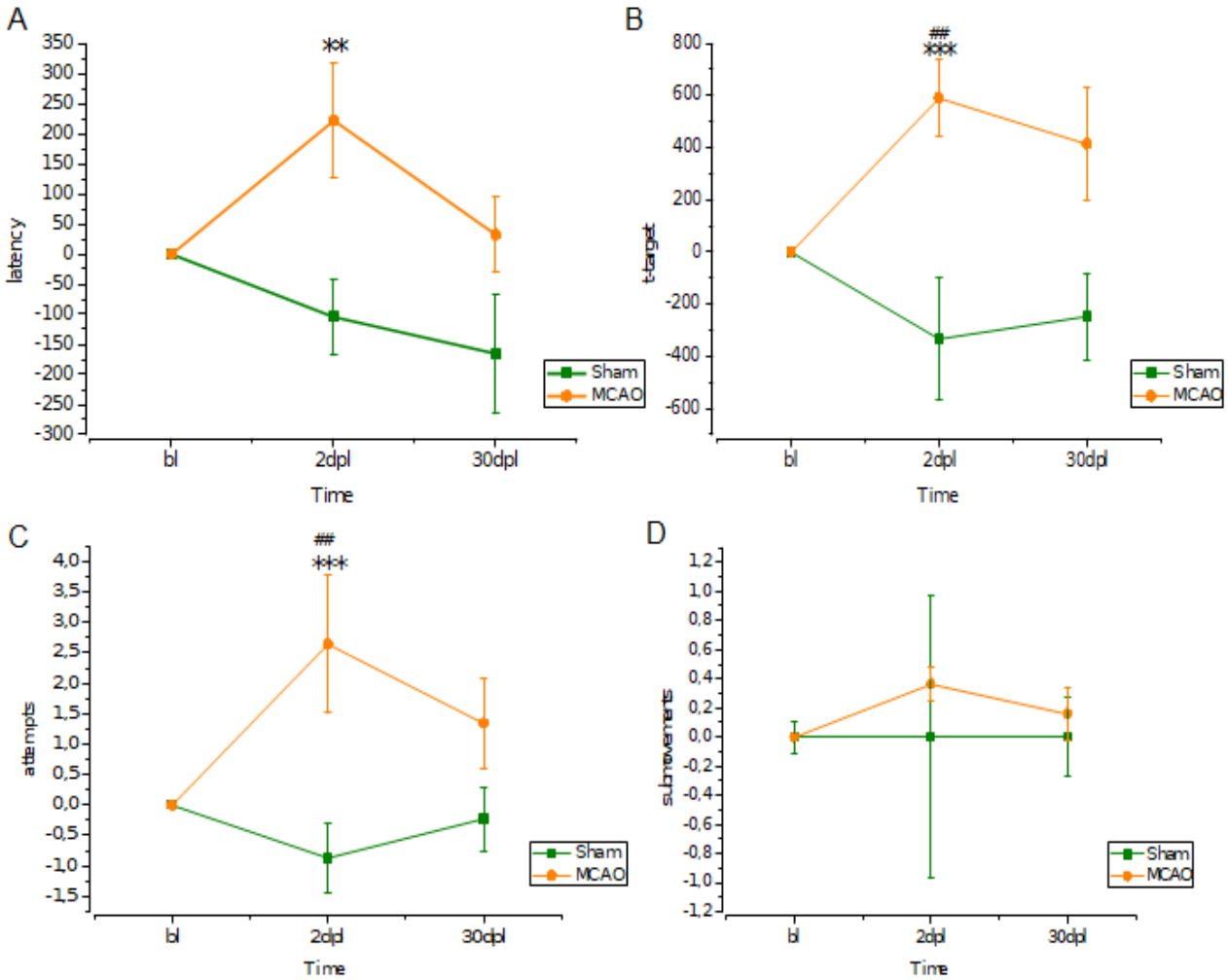

Figure3. 9: Analysis of robot task performance. ***(A)*** *Latency.* ***(B)*** *T-target.* ***(C)*** *Attempts.* ***(D)*** *Submovements. (*) represents significant difference from the baseline, ***, p < 0.001,**, p<0.01. '#' represents significant difference from the sham group, ###, p < 0.001, ##, p<0.01 (n=29; MCAO=16, sham=13).*

We observed that the difference between 2dpl and baseline performance was significantly higher in MCAO animals than in sham for latency, t-target and attempts. Indeed, the MCAO group took longer to start performing the task **(Figure 3.9 A)**, spent more time to accomplish the retraction task **(Figure 3.9 B)** and made more attempts (abortive tries not resulting in a movements) at 2dpl showing an improvement trend at 30dpl **(Figure 3.9 C)**.We did not found statistically difference in the number of submovements.**(Figure 3.9 D)**. We also observed a progressive improvement in the performance of the sham group, probably due to learning.

The M-platform allows also to perform an isometric task (45s of duration), in which the forelimb is kept extended and the amplitude of the exerted force and its relative area-under-the-curve (AUC) of each peak was measured with the idea of evaluating the maximum force of the animal **(Figure 3.10)**. Even in this case, sham animals (n=12) tended to improve their performance in terms of force peak amplitude, reaching the statistical significance at 2dpl. By contrast MCAO group (n=16) reduced its performance soon after the lesion and continue to reduce its force peak at 30dpl **(Figure 3.10 A)**. Coherently, the AUC parameter significantly decreased 2 days post-stroke and remained significantly affected up to 30dpl **(Figure 3.10 B)**.

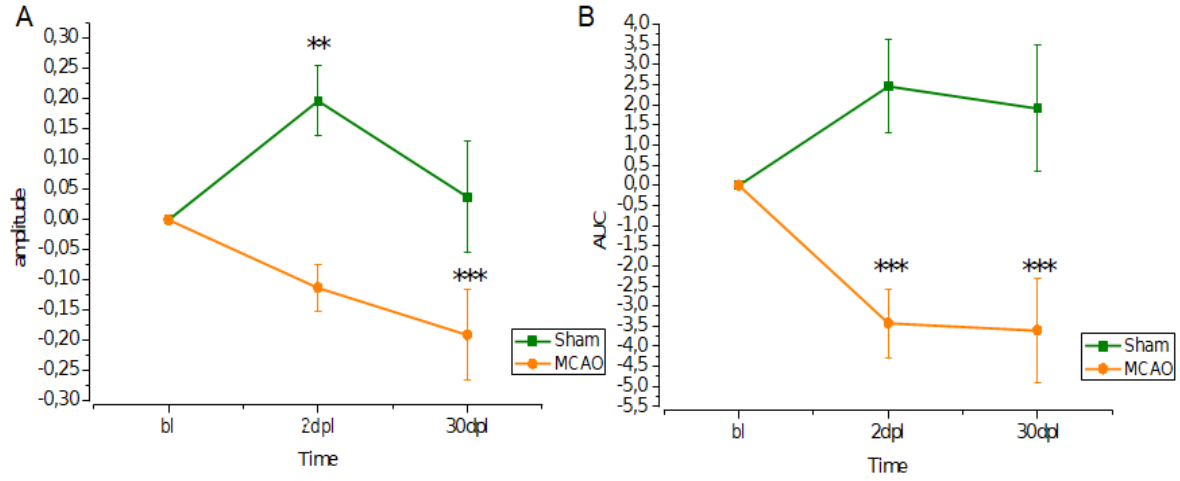

Figure3. 10: Analysis of isometric performance. (A) *Amplitude.* ***(B)*** *AUC. (*) represents significant difference from the baseline, ***, p < 0.001,**, p<0.01 (n=29; MCAO=16, sham=12).*

To combine all behavioural results a novel motor score was established including all motor tests together for the different time-points considered. For this, performance relative to each behavioural tests was converted in a range from 0 to 10 (see Materials and Methods). The differences between sham (n=12) and MCAO groups (n=22) were showed as a radar plot, where each test is represented on one axis. We observed a retraction of the plotted orange area in MCAO group due to loss of motor function, while the green plot relative to sham group remained almost unchanged over time **(Figure 3.11)**.

Figure3. 11: Motor score. *MCAO and sham motor score for all time-points considerate (n=34; MCAO=22, sham=12).*

Then, we have calculated the total score as a sum of total of converted points, mimicking what is done with clinical scales for humans. We quantified a significant decrease of the overall motor function in the MCAO animals at 2dpl with a trend of improvement observed at 30dpl **(Figure 3.12)**. To the contrary, sham animals showed no longitudinal differences in the overall motor performance.

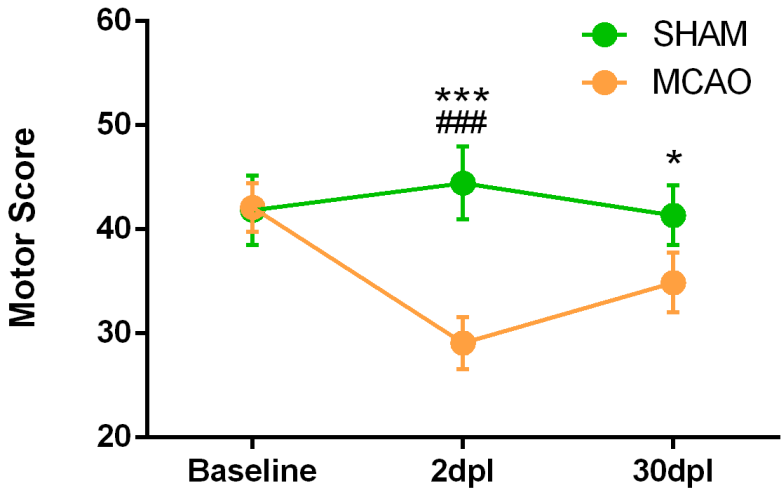

Figure3. 12: Motor score sum.(*) represents significant difference from the baseline, ***, p < 0.001,*, p < 0.05. '#' represents significant difference from the sham group, ###, p < 0.001 (n=34; MCAO=22, sham=12).

3.3 Proportional recovery in MCAO model

Since our starting goal was to establish a stroke model characterized by a large variability in order to mimic the human stroke condition, where a proportional recovery rules has been observed, we evaluated if animals in our MCAO groups (n=13) followed a proportional recovery as well as in humans. Firstly we considered the global motor score including the performance of all used motor tests. We found that after normalizing performance on the baseline values, the acute motor function (assessed at 2 days after stroke) was greatly variable among animals showing a range of motor deficit going from a really mild (acute performance close to 100%) to a really severe (close to 0%) impairment. Moreover, we found that some mice increased their global motor performance at 30 days post lesion **(Figure 3.13 light red)** while other mice not recovered or even worsened their motor function in the chronic phase **(Figure 3.13 red)**.

Thus it is possible to subdivide our ischemic animals in good or poor recovers strengthening the similarity with human stroke patients.

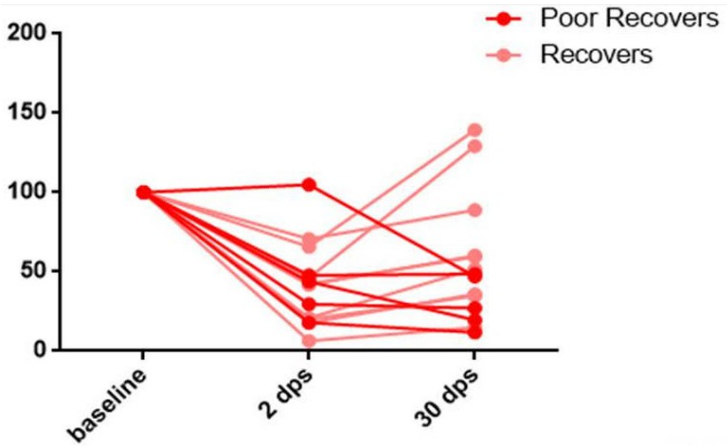

Figure3. 13: Recovery trend in MCAO group. *In the y axis % of pre-stroke performance. In the x axis recovery after stroke for each animal (n=13).*

Given that it has been suggested that the acute deficit could be a strong predictor of chronic motor improvement in humans, we assessed whether a correlation among acute and chronic performance was evident in our data (n=13). We obtained acute performance by subtracting the baseline from performance at day 2, while chronic performance was obtained by subtracting the baseline from day 30 its baseline. Interestingly, we found a positive correlation between the acute and the chronic global motor performance, making the early deficit as a good predictor of final motor outcome as well as in humans **(Figure 3.14)**.

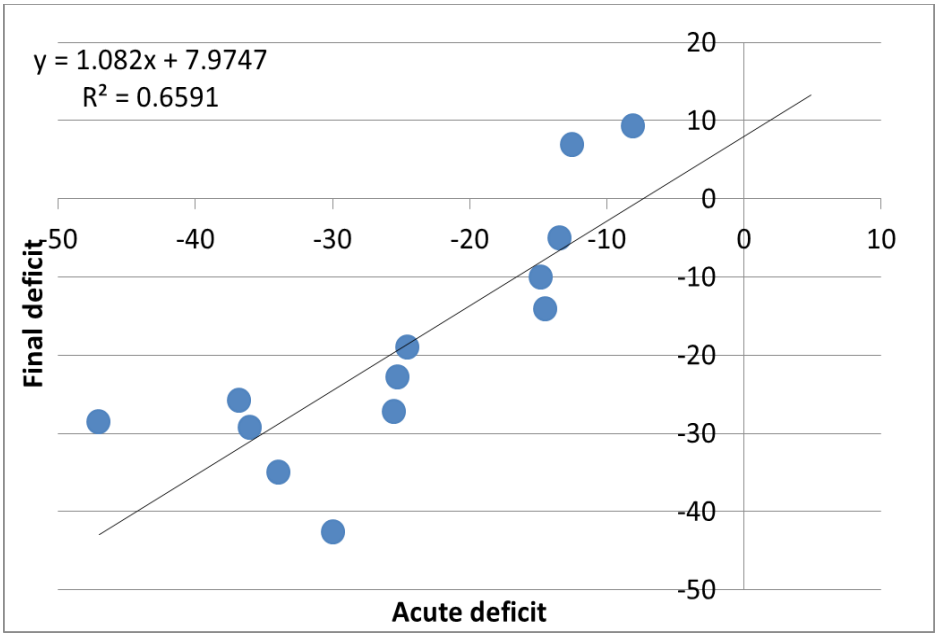

Figure3. 14: Acute deficit trend in MCAO group *(n=13). In the x axis initial deficit of acute phase, in the y axis final deficit in chronic phase.*

3.4 Preliminary correlation between functional and anatomical changes

We were also interested in evaluating if anatomical parameters could predict motor outcome in the acute and chronic phases. Thus, we performed simple linear regressions among the performance of the animals analysed in different behavioural tasks and each anatomical change we quantified (n=15). We found a good trend between the score obtained in the reaching test and the volume of the lesion **(Figure 3.15)**.

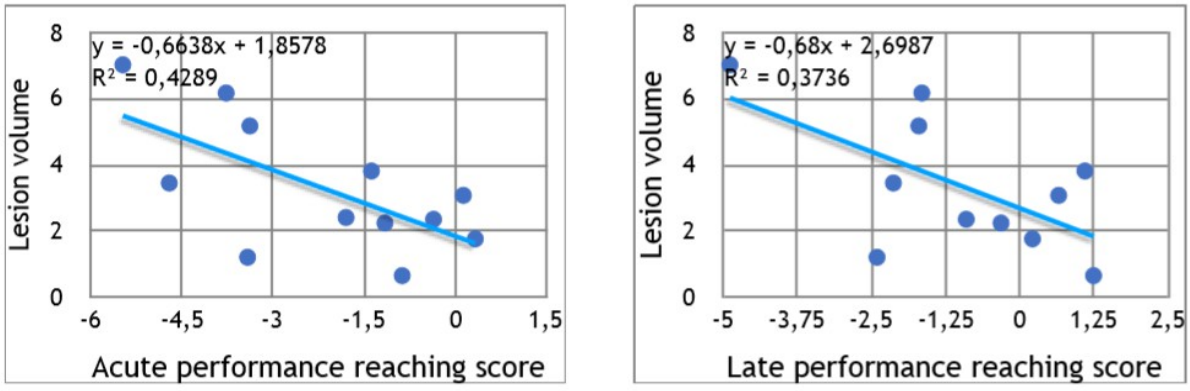

Figure3. 15: Linear regression between reaching test and lesion volume. *Regression between acute or late performance in reaching task and lesion volume in mice underwent MCAO. (n=15).*

The data also seems to correlated in only the animals with the injured CFA were considered (n=5). Instead, no robust correlations have been found in animals with intact CFA **(Figure 3.16)**.

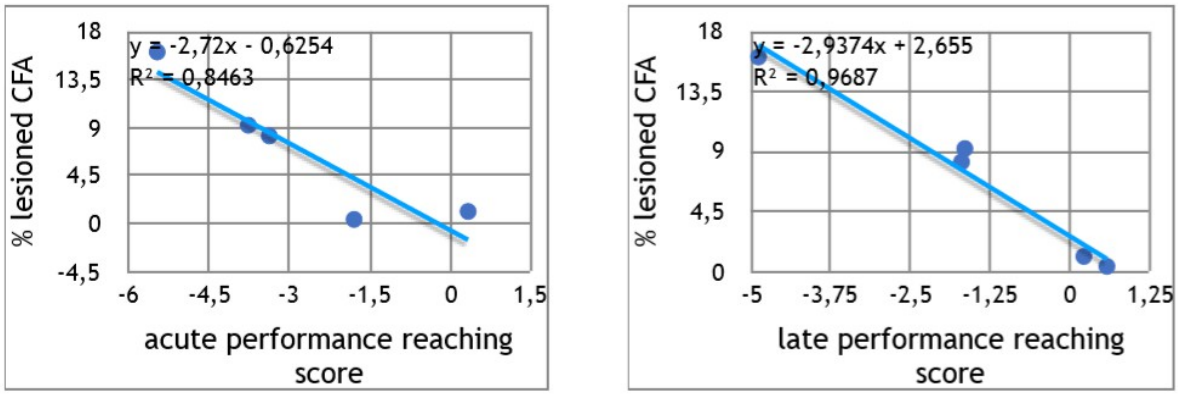

Figure3. 16: Linear regression between reaching test and CFA lesioned mice. *Regression between acute or late performance in reaching task and lesion volume or the percentage of lesioned CFA in MCAO mice that repeated a robust damage on the CFA (n=5).*

Among animals with CFA damage we also found that the acute (but not chronic performance) in the isometric task has a tendency both with the % of lesioned CFA **(Figure 3.17 A)** and with the volume of the lesion **(Figure 3.17 B)**, confirming that anatomical parameters could be good biomarkers of post-stroke motor function.

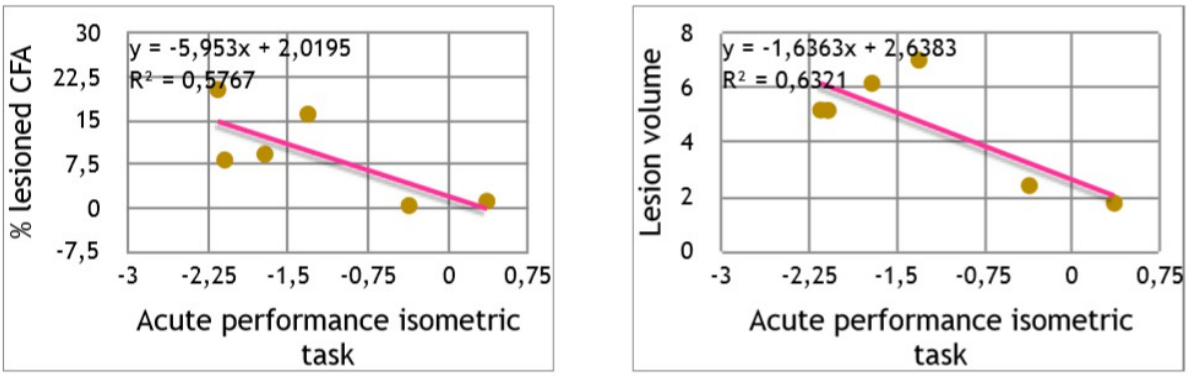

Figure3. 17: Linear regression between isometric task and CFA, volume lesioned mice. *Regression between isometric task acute performance and lesion volume or percentage of lesioned CFA in MCAO mice that showed a robust damage on the CFA (n=5).*

3.5 Electrophysiological alterations after MCAO

3.5.1 MCAO-induced power spectral density changes

Since MCAO spares most of the area of the CFA, the MCAO model allows to study electrophysiological alterations in this region and to link them to the behavioural outcome. So, in order to identify possible predictors of functional outcome after stroke, we started to consider if induction of MCAO produced measurable electrophysiological changes. For this purpose, we recorded neural signals from animals in freely moving condition by means of chronic electrodes implanted bilaterally in the CFA. The recordings were made longitudinally before the induction of the stroke and then at 2, 16 and 30dpl, analysing power spectral density in standard electrophysiological bands (delta, theta, alpha, beta and gamma, see Materials and Methods).

In the MCAO group we observed a significant decrease in the ipsi/contra ratio of the beta power at 16dpl that further decreased at 30dpl, while for the sham group we did not observe changes for any of the spectral bands **(Figure 3.18)**.

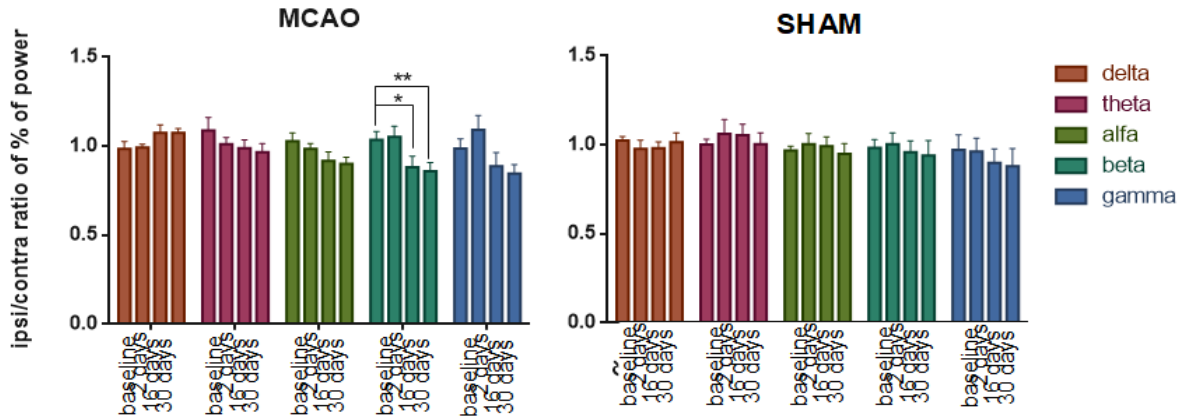

Figure3. 18: EEG power spectral density changes after MCAO induction. *Time course of power spectral density for standard electrophysiological bands. '*' represents significant difference from the baseline, **, p < 0.01, *, p < 0.05 (n=29; MCAO=16, sham=13).*

In particular, looking at changes occurring in the single ipsilateral and contralateral hemispheres of MCAO animals **(Figure 3.19)**, we found a progressive decrease in the power of the theta, beta and gamma bands in the affected hemisphere. In addition, we noticed an increase in the delta spectrum, which reached a statistical significance at 2dpl.

For the healthy hemisphere, we observed significant changes at 2dpl for the gamma band but also, a total reestablishment in the following days.

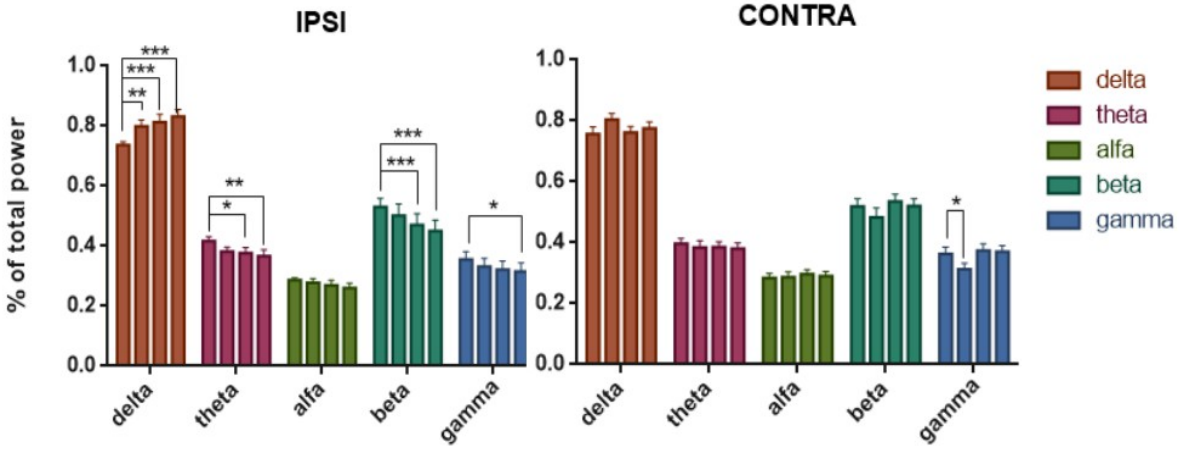

Figure3. 19: EEG power spectral density changes in MCAO group. *Time course of power spectral density for standard electrophysiological bands in the affected and healthy hemisphere, respectively. '*' represents significant difference from the baseline, ***, p < 0.001, **, p < 0.01, *, p < 0.05 (n=16).*

3.5.2 Preliminary evaluation of electrophysiological changes in the M-platform

Recordings of local field potentials (LFPs) were also performed from both hemispheres during the retraction task in the M-Platform. Since we wanted to better characterize electrophysiological events that were associated with the generation of a force peak onto the M-platform, in order to study them in the context of MCAO, we measured the amplitude of event-related potentials (ERPs obtained by aligning neural signals on the start of each force peaks measured in the M-Platform) **(Figure 3.20)**. In naïve conditions, a well-defined ERP is easily detectable, showing an early positive and late negative phases. Stroke had a deleterious impact on the ERP shape, abolishing both the early and late components at 2dpl (red trace) **(Figure 3.20 A)** The quantification of the peak-to-paek amplitude confirmed a significant decrease at 2 days after stroke with a partial recovery of the ERP amplitude 16 and 30 days following the injury **(Figure 3.20 B)**.

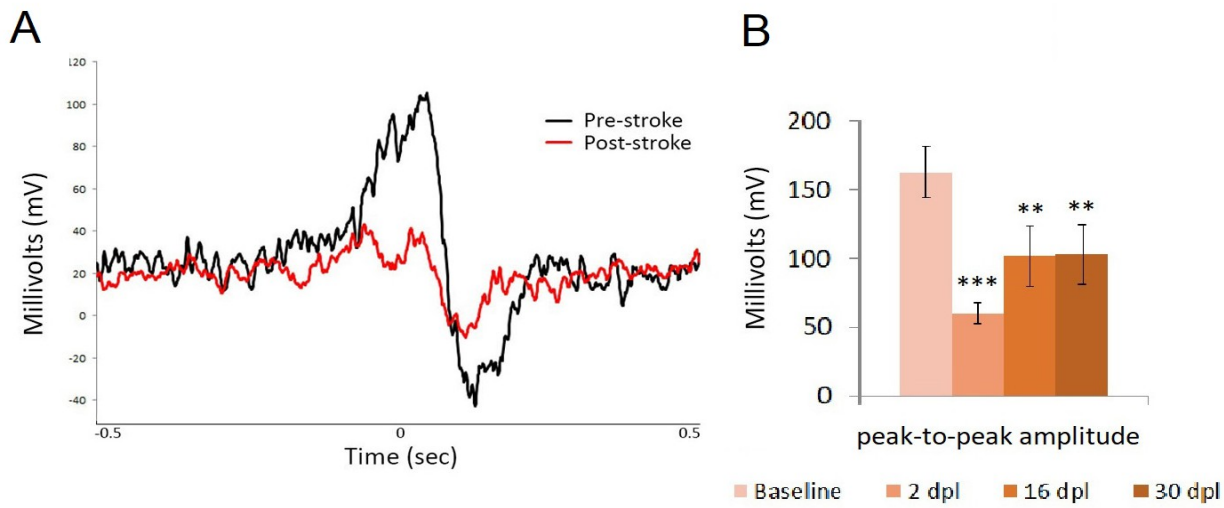

Figure3. 20: Post-stroke evolution of electrophysiological parameters. (A) *Representative traces of the Event Related Potentials (ERP) aligned on the onset of the force peak.* ***(B)*** *Longitudinal variation of ERP amplitude in the ipsilesional hemisphere at different times after stroke (n=8).*

Chapter 4. Discussion

4.1 Anatomical and behavioural changes in MCAO induction

Stroke is a highly variable condition in stroke patients and functional outcomes strongly depends of many factors. In this context, the MCAO is a suitable model because it is similar to the human condition. In fact, we have found that the lesion varied significantly in terms of extension and localization **(Figure 3.2)**. We also demonstrated that the focal site of the lesion involved predominantly somatosensory areas, whereas the motor areas, including the CFA, were only partially affected or represented a perilesional site. Indeed, only a minority of animals showed a robust damage in the CFA **(Figure 3.4)**. As expected, the impairment of the CFA was associated with larger lesions. MCAO-induced lesion also provoked an imbalance in the integrity of the white matter, especially for the external capsule. Anatomical alterations reflects in a loss of the contralateral forelimb motor function. In fact, permanent MCAO determines a clear motor deficit at the level of the contralesional forelimb, as we could observe in the gridwalk test **(Figure 3.8)**.

However, forelimb motor deficit extends beyond what can be assessed by means of gridwalk test, in fact we could measure an impairment in the performance, during fine grasping behavior by means of the skilled reaching test. Fine grasping behaviour spontaneously recovered in the chronic phase **(Figure 3.7).** This is in keeping with the idea that a damage of somatosensory areas may deprive motor cortex of important inputs for motor adaptation and coordination (Mathis et al. 2017), but that subsequent plastic phenomena can improve the overall function probably via recruiting compensatory strategies.

We also utilized the M-platform **(Figure 2.8)** to characterise the motor deficit associated with MCAO (Spalletti et al. 2014). In this case, the M-platform was not used for rehabilitation, instead, we exploited this tool for its ability to extract kinetic and kinematic parameters of the retraction movement. Also, the M-platform allows to perform an isometric task, which provides additional parameters associated with the maximal force the animals is able to generate. Kinetic and kinematic features of the motor performance during robotic tasks, showed a large panel of motor outcome in the late phase, with a complete, mild or without any degree of recovery (**Figure 3.9, 3.10**).Together with a deficit in the performance of MCAO group on the robotic platform we observed an increase in the performance of sham animals probably due to learning **(Figure 3.9)**.

Mimicking clinical scale for humans, in this thesis we also implemented a novel global motor score (**Figure 3.11**) accounting for all the motor performance evaluated in the single motor tests. This general motor score showed a significant drop in the overall motor performance of MCAO mice, respect both baseline condition and sham animals (**Figure 3.12**). Consistently with the functional improvement observed in the skilled reaching test and in some kinetic parameters relative to the robotic task, MCAO mice showed an significative increment in their performance at 30 days post lesion.

4.2 Proportional recovery and preliminary correlation analysis

The proportional recovery rule has been confirmed in the motor domain several times. Evidence also suggests that proportional recovery applies to non-motor areas, such as language (Lazar et al. 2010) and hemispatial neglect (Nijboer et al. 2013). Moreover, these recent findings suggest that studies exploring the effect of any post-stroke therapy need to be contextualized in a proportional recovery framework. This striking clinical phenomenon provides a framework for investigating potentially modifiable biological factors that are necessary for maximizing recovery of function and raises several clinical questions: (i) can we help patients with stroke to regain more than 70% of lost function and how, (ii) can we predict the long-term motor outcome, regardless the initial impairment, (iii) can we predict if a patient will respond to a treatment, in order to customize the therapy and (iv) how can we turn poor recovers into proportional recovers?

In this project, we laid the bases to investigate biomarkers that can help predicting whether proportional recover will occur or not.

For this we needed a preclinical model characterized by such variability. The MCAO procedure produces a large ischaemic lesion, the size of which is consistent with what is reported in the literature (e.g. Llovera et al. 2014), but varies significantly in terms of extension and localization. In addition, the lesion edges are difficult to identify due to a gradual decline in neuronal density from the ischemic nucleus to the healthy tissue, which is consistent with the established presence of a penumbra in this model (Carmichael et al. 2005). Both these aspects make the MCAO model similar to the human condition.

Thus, we verify if MCAO mice showed different inter-individual degree of recovery. Interestingly, we found a segregation of poor and good recovers **(Figure 3.13)**, meaning that some animals recovered while others maintained their deficits.

Making advantage of this observed variability, we conducted a preliminary linear regression analysis between anatomical measures and indices of motor recovery in our set of behavioural tests. First of all we confirmed, as previously reported in the literature, that the extent of the acute deficit is a good predictor for the late motor performance **(Figure 3.14)**. The second aspect emerging from our data is that the also the lesion extension, and particularly the eventual involvement of the CFA, can give valuable prediction of motor performance both in the skilled reaching test and in the isometric task **(Figure 3.15, 3.16, 3.17)**.

In the future, we will perform more sophisticated statistical analyses to assess the predictive power of our parameters.

4.3 Post-stroke electrophysiological alterations

In parallel with behavioural tests, we performed also electrophysiological measures both in freely moving condition and during the retraction task onto the M-platform. For the freely moving condition, we performed a standard analysis of the relative power of electrophysiological spectral bands. We observed affected hemisphere-specific alterations in the power spectrum, in particular a decrease in the beta, theta and gamma bands and an increase in the delta band **(Figure 3.19)**. It has been frequently reported, both in humans and in rodents, that an increase in slow waves and a decrease in rapid waves take place after stroke, i.e. increment of delta band and decline of beta bands observed in our experiments.

We characterised also the event-related potential (ERP) associated with forelimb retraction **(Figure 3.17)**. Even in this case, we observed clear alterations after stroke. In particular, the reduced amplitude of the peaks could be associated with a damaging of feed-forward connections from the somatosensory cortex (Petrof et al. 2015). Currently, we are analysing inter-hemispheric interactions, which can be easily implemented given our set up of bilateral electrode recordings. Particularly, we are using different quantitative methods of time series analysis, e.g. cross-correlation and mutual information. Moreover, once completed, we will use our panel of electrophysiological measures to conduct multiple regression together with anatomical predictors, in order to delineate a possible combination of anatomo-physiological factors useful to early predict the late motor recovery.

References

Aho, K., Harmsen, P., Hatano, S., Marquardsen, J., Smirnov, V., Strasser, T. (1980). Cerebrovascular disease in the community: results of a WHO collaborative study. *Bull World Health Organ*, pp.113–130.

Alia, C., Spalletti, C., Lai, S., Panarese, A., Micera, S. and Caleo, M. (2016). Reducing GABAA-mediated inhibition improves forelimb motor function after focal cortical stroke in mice. *Scientific Reports*, 6(1).

Alix, J. (2006). Recent Biochemical Advances in White Matter Ischaemia. *European Neurology*, 56(2), pp.74-77.

Allred, R., Cappellini, C. and Jones, T. (2010). The “good” limb makes the “bad” limb worse: Experience-dependent interhemispheric disruption of functional outcome after cortical infarcts in rats. *Behavioral Neuroscience*, 124(1), pp.124-132.

Amarenco, P., Bogousslavsky, J., Caplan, L., Donnan, G. and Hennerici, M. (2009). Classification of Stroke Subtypes. *Cerebrovascular Diseases*, 27(5), pp.493-501.

Arumugam, T., Baik, S., Balaganapathy, P., Sobey, C., Mattson, M., Jo, D. (2018). Notch signaling and neuronal death in stroke. *Progress in Neurobiology*, pp.103-116.

Baldassarre, A., Ramsey, L., Rengachary, J., Zinn, K., Siegel, J., Metcalf, N., Strube, M., Snyder, A., Corbetta, M. and Shulman, G. (2016). Dissociated functional connectivity profiles for motor and attention deficits in acute right-hemisphere stroke. *Brain*, 139(7), pp.2024-2038.

Baptista, D., Abreu, P., Azevedo, E., Magalhães, R. and Correia, M. (2018). Sex Differences in Stroke Incidence in a Portuguese Community-Based Study. *Journal of Stroke and Cerebrovascular Diseases*, 27(11), pp.3115-3123.

Barker-Collo, S., Bennett, D., Krishnamurthi, R., Parmar, P., Feigin, V., Naghavi, M., Forouzanfar, M., Johnson, C., Nguyen, G., Mensah, G., Vos, T., Murray, C. and Roth, G. (2015). Sex Differences in Stroke Incidence, Prevalence, Mortality and Disability-Adjusted Life Years: Results from the Global Burden of Disease Study 2013. *Neuroepidemiology*, 45(3), pp.203-214.

Barreto, G., Sun, X., Xu, L. and Giffard, R. (2011). Astrocyte Proliferation Following Stroke in the Mouse Depends on Distance from the Infarct. *PLoS ONE*, 6(11), p.e27881.

Bartos, M., Vida, I. and Jonas, P. (2007). Synaptic mechanisms of synchronized gamma oscillations in inhibitory interneuron networks. *Nature Reviews Neuroscience*, 8(1), pp.45-56.

Bembenek, J., Kurczych, K., Karlinski, M. and Czlonkowska, A. (2013). P 78. The prognostic value of motor-evoked potentials in motor recovery and functional outcome after stroke – a systematic review of the literature. *Clinical Neurophysiology*, 124(10), p.e103.

Berlucchi, G. (2011). Brain plasticity and cognitive neurorehabilitation. *Neuropsychological Rehabilitation*, 21(5), pp.560-578.

Bernhardt, J., Hayward, K., Kwakkel, G., Ward, N., Wolf, S., Borschmann, K., Krakauer, J., Boyd, L., Carmichael, S., Corbett, D. and Cramer, S. (2017). Agreed definitions and a shared vision for new standards in stroke recovery research: The Stroke Recovery and Rehabilitation Roundtable taskforce. *International Journal of Stroke*, 12(5), pp.444-450.

Berretta, A., Tzeng, Y. and Clarkson, A. (2014). Post-stroke recovery: the role of activity-dependent release of brain-derived neurotrophic factor. *Expert Review of Neurotherapeutics*, 14(11), pp.1335-1344.

Biernaskie, J. (2004). Efficacy of Rehabilitative Experience Declines with Time after Focal Ischemic Brain Injury. *Journal of Neuroscience*, 24(5), pp.1245-1254.

Biernaskie, J., Szymanska, A., Windle, V. and Corbett, D. (2005). Bi-hemispheric contribution to functional motor recovery of the affected forelimb following focal ischemic brain injury in rats. *European Journal of Neuroscience*, 21(4), pp.989-999.

Bigourdan, A., Munsch, F., Coupé, P., Guttmann, C., Sagnier, S., Renou, P., Debruxelles, S., Poli, M., Dousset, V., Sibon, I. and Tourdias, T. (2016). Early Fiber Number Ratio Is a Surrogate of Corticospinal Tract Integrity and Predicts Motor Recovery After Stroke. *Stroke*, 47(4), pp.1053-1059.

Broeks, G., Lankhorst, J., Rumping,G., Prevo, K. and A. (1999). The long-term outcome of arm function after stroke: results of a follow-up study. *Disability and Rehabilitation*, 21(8), pp.357-364.

Burghaus, L., Burghaus, L., Dohmen, C., Bosche, B., Galldiks, N., Winhuisen, L., Szelies, B. and Haupt, W. (2006). Early Electroencephalography in Acute Ischemic Stroke: Prediction of a Malignant Course?. *Klinische Neurophysiologie*, 37(01).

Burke Quinlan, E., Dodakian, L., See, J., McKenzie, A., Le, V., Wojnowicz, M., Shahbaba, B. and Cramer, S. (2014). Neural function, injury, and stroke subtype predict treatment gains after stroke. *Annals of Neurology*, 77(1), pp.132-145.

Byblow, W., Stinear, C., Barber, P., Petoe, M. and Ackerley, S. (2015). Proportional recovery after stroke depends on corticomotor integrity. *Annals of Neurology*, 78(6), pp.848-859.

Calautti, C. and Baron, J. (2003). Functional Neuroimaging Studies of Motor Recovery After Stroke in Adults. *Stroke*, 34(6), pp.1553-1566.

Caplan, L. Simon, R. (2015). Chapter 22 - Cerebrovascular Disease – Stroke. *Neurobiology of Brain Disorders*, p. 339-355.

Carmichael, S. (2005). Rodent models of focal stroke: Size, mechanism, and purpose. *NeuroRX*, 2(3), pp.396-409.

Carter, A., Astafiev, S., Lang, C., Connor, L., Rengachary, J., Strube, M., Pope, D., Shulman, G. and Corbetta, M. (2009). Resting state inter-hemispheric fMRI connectivity predicts performance after stroke. *Annals of Neurology*.

Chang, M., Do, K. and Chun, M. (2015). Prediction of lower limb motor outcomes based on transcranial magnetic stimulation findings in patients with an infarct of the anterior cerebral artery. *Somatosensory & Motor Research*, 32(4), pp.249-253.

Chen, G., Zhang, Y., Li, X., Zhao, X., Ye, Q., Lin, Y., Tao, H., Rasch, M. and Zhang, X. (2017). Distinct Inhibitory Circuits Orchestrate Cortical beta and gamma Band Oscillations. *Neuron*, 96(6), pp.1403-1418.e6.

Cicinelli, P., Pasqualetti, P., Zaccagnini, M., Traversa, R., Oliveri, M. and Rossini, P. (2003). Interhemispheric Asymmetries of Motor Cortex Excitability in the Postacute Stroke Stage. *Stroke*, 34(11), pp.2653-2658.

Cicinelli, P., Traversa, R. and Rossini, P. (1997). Post-stroke reorganization of brain motor output to the hand: a 2–4 month follow-up with focal magnetic transcranial stimulation. *Electroencephalography and Clinical Neurophysiology/Electromyography and Motor Control*, 105(6), pp.438-450.

Clarkson et al., “AMPA Receptor-Induced Local Brain-Derived Neurotrophic Factor Signaling Mediates Motor Recovery after Stroke”. (2017). *The Journal of Neuroscience*, 37(42), pp.10252-10252.

Clarkson, A., Huang, B., MacIsaac, S., Mody, I. and Carmichael, S. (2010). Reducing excessive GABA- mediated tonic inhibition promotes functional recovery after stroke. *Nature*, 468(7321), pp.305-309.

Coupar, F., Pollock, A., Rowe, P., Weir, C. and Langhorne, P. (2011). Predictors of upper limb recovery after stroke: a systematic review and meta-analysis. *Clinical Rehabilitation*, 26(4), pp.291-313.

Coupland, A., Thapar, A., Qureshi, M., Jenkins, H. and Davies, A. (2017). The definition of stroke. *Journal of the Royal Society of Medicine*, 110(1), pp.9-12.

Cramer, S. (2008). Repairing the human brain after stroke: I. Mechanisms of spontaneous recovery. *Annals of Neurology*, 63(3), p. 272-287.

Cramer, S., Koroshetz, W. and Finklestein, S. (2007). The Case for Modality-Specific Outcome Measures in Clinical Trials of Stroke Recovery-Promoting Agents. *Stroke*, 38(4), pp.1393-1395.

Dirnagl, A., Iadecola, C., Moskowitz, M. (1999). Pathobiology of ischemic stroke: an integrated view. *Trends in Neurosciences,* 22(9), pp.392-397.

Dong, Y., Dobkin, B., Cen, S., Wu, A. and Winstein, C. (2006). Motor Cortex Activation During Treatment May Predict Therapeutic Gains in Paretic Hand Function After Stroke. *Stroke*, 37(6), pp.1552-1555.

Dorrance, A., Fink, G. (2015). Effects of Stroke on the Autonomic Nervous System. *Comprehensive Physiology,* pp.1241–1263.

Durukan, A. and Tatlisumak, T. (2007). Acute ischemic stroke: Overview of major experimental rodent models, pathophysiology, and therapy of focal cerebral ischemia. *Pharmacology Biochemistry and Behavior*, 87(1), pp.179-197.

Emmons, E., Ruggiero, R., Kelley, R., Parker, K. and Narayanan, N. (2016). Corticostriatal Field Potentials Are Modulated at Delta and Theta Frequencies during Interval-Timing Task in Rodents. *Frontiers in Psychology*, 7.

Feigin, V. (2019). Anthology of stroke epidemiology in the 20th and 21st centuries: Assessing the past, the present, and envisioning the future. *International Journal of Stroke*, p.174749301983299.

Feng, W., Wang, J., Chhatbar, P., Doughty, C., Landsittel, D., Lioutas, V., Kautz, S. and Schlaug, G. (2015). Corticospinal tract lesion load: An imaging biomarker for stroke motor outcomes. *Annals of Neurology*, 78(6), pp.860-870.

Feydy, A., Carlier, R., Roby-Brami, A., Bussel, B., Cazalis, F., Pierot, L., Burnod, Y. and Maier, M. (2002). Longitudinal Study of Motor Recovery After Stroke. *Stroke*, 33(6), pp.1610-1617.

Finnigan, S. and van Putten, M. (2013). EEG in ischaemic stroke: Quantitative EEG can uniquely inform (sub-)acute prognoses and clinical management. *Clinical Neurophysiology*, 124(1), pp.10-19.

Finnigan, S., Wong, A. and Read, S. (2016). Defining abnormal slow EEG activity in acute ischaemic stroke: Delta/alpha ratio as an optimal QEEG index. *Clinical Neurophysiology*, 127(2), pp.1452-1459.

Frost, S., Barbay, S., Friel, K., Plautz, E. and Nudo, R. (2003). Reorganization of Remote Cortical Regions After Ischemic Brain Injury: A Potential Substrate for Stroke Recovery. *Journal of Neurophysiology*, 89(6), pp.3205-3214.

Fu, Y., Kaneko, M., Tang, Y., Alvarez-Buylla, A. and Stryker, M. (2015). A cortical disinhibitory circuit for enhancing adult plasticity. *eLife*, 4.

Gillbert, C., Humphreys, G., Mantini, D. (2014). Automated delineation of stroke lesions using brain CT images. *NeuroImage: Clinical,* pp.540-548.

Hankey, G. (2017). Stroke. *The Lancet*, 389(10069), pp.641-654.

Hankey, G. and Blacker, D. (2015). Is it a stroke?. *BMJ*, 350(jan15 1), pp.h56-h56.

Harrison, T., Silasi, G., Boyd, J. and Murphy, T. (2013). Displacement of Sensory Maps and Disorganization of Motor Cortex After Targeted Stroke in Mice. *Stroke*, 44(8), pp.2300-2306.

Heald, A., Bates, D., Cartlidge, N., French, J. and Miller, S. (1993). Longitudinal study of central motor conduction time following stroke: 2. Central motor conduction measured within 72 h after stroke as a predictor of functional outcome at 12 months. *Brain*, 116(6), pp.1371-1385.

Helenius, J. and Henninger, N. (2015). Leukoaraiosis Burden Significantly Modulates the Association Between Infarct Volume and National Institutes of Health Stroke Scale in Ischemic Stroke. *Stroke*, 46(7), pp.1857-1863.

Hofmeijer, J. and van Putten, M. (2012). Ischemic Cerebral Damage. *Stroke*, 43(2), pp.607-615.

Hort, I. and Karenberg, A. (1998). Medieval Descriptions and Doctrines of Stroke: Preliminary Analysisof Select Sources. Part I: The Struggle for Terms and Theories - Late Antiquityand Early Middle Ages (300-800). *Journal of the History of the Neurosciences*, 7(3), pp.162-173.

Igarashi, J., Isomura, Y., Arai, K., Harukuni, R. and Fukai, T. (2013). A θ–γ Oscillation Code for Neuronal Coordination during Motor Behavior. *Journal of Neuroscience*, 33(47), pp.18515-18530.

Jesen, O., Goel, P., Kopell, N., Pohja, M., Hari, R. and Ermentrout, B. (2005). On the human sensorimotor-cortex beta rhythm: Sources and modeling. *NeuroImage*, 26(2), pp.347-355.

Johnson, N., Özkan, M., Burgess, A., Prokic, E., Wafford, K., O'Neill, M., Greenhill, S., Stanford, I. and Woodhall, G. (2017). Phase-amplitude coupled persistent theta and gamma oscillations in rat primary motor cortex in vitro. *Neuropharmacology*, 119, pp.141-156.

Johnson, W., Onuma, O., Owolabi, M. and Sachdev, S. (2016). Stroke: a global response is needed. *Bulletin of the World Health Organization*, 94(9), pp.634-634A.

Karenberg, A. and Moog, F. (1997). Apoplexy in ancient medical writing. F*ortschritte der Neurologie · Psychiatrie*, 65(11), pp.489-503.

Karthikeyan, S., Jeffers, M., Carter, A. and Corbett, D. (2018). Characterizing Spontaneous Motor Recovery Following Cortical and Subcortical Stroke in the Rat. *Neurorehabilitation and Neural Repair*, 33(1), pp.27-37.

Kim, J. and Caplan, L. (2016). Clinical Stroke Syndromes. *Intracranial Atherosclerosis: Pathophysiology, Diagnosis and Treatment*, 40, pp.72–92.

Kleim, J., Boychuk, J. and Adkins, D. (2007). Rat Models of Upper Extremity Impairment in Stroke. *ILAR Journal*, 48(4), pp.374-385.

Kraemer, M., Schormann, T., Hagemann, G., Qi, B., Witte, O. and Seitz, R. (2004). Delayed Shrinkage of the Brain After Ischemic Stroke: Preliminary Observations With Voxel-Guided Morphometry. *Journal of Neuroimaging*, 14(3), pp.265-272.

Krakauer, J. and Marshall, R. (2015). The proportional recovery rule for stroke revisited. *Annals of Neurology*, 78(6), pp.845-847.

Krnjević, K. (2008). Electrophysiology of cerebral ischemia. *Neuropharmacology*, 55(3), pp.319-333.

Kroemer, G. (2001). Mitochondrial control of cell death. *The Scientific World JOURNAL*, 1(S3), pp.48-48.

Kumar, S., & Caplan, L. R. (2007). Why identification of stroke syndromes is still important. *Current Opinion in Neurology, 20(1), 78–82.*

Kwakkel, G., Kollen, B., van der Grond, J. and Prevo, A. (2003). Probability of Regaining Dexterity in the Flaccid Upper Limb. *Stroke*, 34(9), pp.2181-2186.

Laaksonen, K., Helle, L., Parkkonen, L., Kirveskari, E., Mäkelä, J., Mustanoja, S., Tatlisumak, T., Kaste, M. and Forss, N. (2013). Alterations in Spontaneous Brain Oscillations during Stroke Recovery. *PLoS ONE*, 8(4), p.e61146.

Lai, C., Wang, C., Tsai, P., Chan, R., Lin, S., Lin, F. and Hsieh, C. (2015). Corticospinal Integrity and Motor Impairment Predict Outcomes After Excitatory Repetitive Transcranial Magnetic Stimulation: A Preliminary Study. *Archives of Physical Medicine and Rehabilitation*, 96(1), pp.69-75.

Lai, S., Panarese, A., Spalletti, C., Alia, C., Ghionzoli, A., Caleo, M. and Micera, S. (2014). Quantitative Kinematic Characterization of Reaching Impairments in Mice After a Stroke. *Neurorehabilitation and Neural Repair*, 29(4), pp.382-392.

Langhorne, P., Coupar, F. and Pollock, A. (2009). Motor recovery after stroke: a systematic review. *The Lancet Neurology*, 8(8), pp.741-754.

Lazar, R., Minzer, B., Antoniello, D., Festa, J., Krakauer, J. and Marshall, R. (2010). Improvement in Aphasia Scores After Stroke Is Well Predicted by Initial Severity. *Stroke*, 41(7), pp.1485-1488.

Leak, R., Zheng, P., Ji, X., Zhang, J. and Chen, J. (2014). From apoplexy to stroke: Historical perspectives and new research frontiers. *Progress in Neurobiology*, 115, pp.1-5.

Levin, M. (1996). Should stereotypic movement synergies in hemiparetic patients be considered adaptive?. *Behavioral and Brain Sciences*, 19(1), pp.79-80.

Li, P. and Murphy, T. (2008). Two-Photon Imaging during Prolonged Middle Cerebral Artery Occlusion in Mice Reveals Recovery of Dendritic Structure after Reperfusion. *journal of Neuroscience*, 28(46), pp.11970-11979.

Li, S. and Carmichael, S. (2006). Growth-associated gene and protein expression in the region of axonal sprouting in the aged brain after stroke. *Neurobiology of Disease*, 23(2), pp.362-373.

Liepert, J., Miltner, W., Bauder, H., Sommer, M., Dettmers, C., Taub, E. and Weiller, C. (1998). Motor cortex plasticity during constraint-induced movement therapy in stroke patients. *Neuroscience Letters*, 250(1), pp.5-8.

Llovera, G., Roth, S., Plesnila, N., Veltkamp, R. and Liesz, A. (2014). Modeling Stroke in Mice: Permanent Coagulation of the Distal Middle Cerebral Artery. *Journal of Visualized Experiments*, (89).

Longa, E., Weinstein, P., Carlson, S. and Cummins, R. (1989). Reversible middle cerebral artery occlusion without craniectomy in rats. *Stroke*, 20(1), pp.84-91.

López-Larraz, E., Montesano, L., Gil-Agudo, Á. and Minguez, J. (2014). Continuous decoding of movement intention of upper limb self-initiated analytic movements from pre-movement EEG correlates. *Journal of NeuroEngineering and Rehabilitation*, 11(1), p.153.

Mansoori, B., Jean-Charles, L., Touvykine, B., Liu, A., Quessy, S. and Dancause, N. (2014). Acute inactivation of the contralesional hemisphere for longer durations improves recovery after cortical injury. *Experimental Neurology*, 254, pp.18-28.

Mathis, M., Mathis, A. and Uchida, N. (2017). Somatosensory Cortex Plays an Essential Role in Forelimb Motor Adaptation in Mice. *Neuron*, 93(6), pp.1493-1503.e6.

Monfils, M., Plautz, E. and Kleim, J. (2005). In Search of the Motor Engram: Motor Map Plasticity as a Mechanism for Encoding Motor Experience. *The Neuroscientist*, 11(5), pp.471-483.

Murase, N., Duque, J., Mazzocchio, R. and Cohen, L. (2004). Influence of interhemispheric interactions on motor function in chronic stroke. *Annals of Neurology*, 55(3), pp.400-409.

Murphy, T. and Corbett, D. (2009). Plasticity during stroke recovery: from synapse to behaviour. *Nature Reviews Neuroscience*, 10(12), pp.861-872.

Nagata, K., Tagawa, K., Hiroi, S., Shishido, F. and Uemura, K. (1989). Electroencephalographic correlates of blood flow and oxygen metabolism provided by positron emission tomography in patients with cerebral infarction. *Electroencephalography and Clinical Neurophysiology*, 72(1), pp.16-30.

Nicolo, P., Rizk, S., Magnin, C., Pietro, M., Schnider, A. and Guggisberg, A. (2015). Coherent neural oscillations predict future motor and language improvement after stroke. *Brain*, 138(10), pp.3048-3060.

Nijboer, T., Kollen, B. and Kwakkel, G. (2013). Time course of visuospatial neglect early after stroke: A longitudinal cohort study. *Cortex*, 49(8), pp.2021-2027.

Nishibe, M., Barbay, S., Guggenmos, D. and Nudo, R. (2010). Reorganization of Motor Cortex after Controlled Cortical Impact in Rats and Implications for Functional Recovery. *Journal of Neurotrauma*, 27(12), pp.2221-2232.

Nouri, S. and Cramer, S. (2011). Anatomy and physiology predict response to motor cortex stimulation after stroke. *Neurology*, 77(11), pp.1076-1083.

Nowak, M., Zich, C. and Stagg, C. (2018). Motor Cortical Gamma Oscillations: What Have We Learnt and Where Are We Headed?. *Current Behavioral Neuroscience Reports*, 5(2), pp.136-142.

Nudo, R. (2007). Post infarct Cortical Plasticity and Behavioural Recovery. *Stroke*, 38(2), p. 840-845.

Nudo, R., Sutherland, D., Masterton, R. (1995). Variation and evolution of mammalian corticospinal somata with special reference to primates. *The Journal of Comparative Neurology, 358(2), pp.181–205.*

Nudo, R., Wise, B., SiFuentes, F. and Milliken, G. (1996). Neural Substrates for the Effects of Rehabilitative Training on Motor Recovery After Ischemic Infarct. *Science*, 272(5269), pp.1791-1794.

Paciaroni, M., Caso, V. and Agnelli, G. (2009). The Concept of Ischemic Penumbra in Acute Stroke and Therapeutic Opportunities. *European Neurology*, 61(6), pp.321-330.

Park, C., Chang, W., Ohn, S., Kim, S., Bang, O., Pascual-Leone, A. and Kim, Y. (2011). Longitudinal Changes of Resting-State Functional Connectivity During Motor Recovery After Stroke. *Stroke*, 42(5), pp.1357-1362.

Pasquini, M., Lai, S., Spalletti, C., Cracchiolo, M., Conti, S., Panarese, A., Caleo, M. and Micera, S. (2018). A Robotic System for Adaptive Training and Function Assessment of Forelimb Retraction in Mice. *IEEE Transactions on Neural Systems and Rehabilitation Engineering*, 26(9), pp.1803-1812.

Pendlebury, S., Blamire, A., Lee, M., Styles, P. and Matthews, P. (1999). Axonal Injury in the Internal Capsule Correlates With Motor Impairment After Stroke. *Stroke*, 30(5), pp.956-962.

Petrof, I., Viaene, A. and Sherman, S. (2015). Properties of the primary somatosensory cortex projection to the primary motor cortex in the mouse. *Journal of Neurophysiology*, 113(7), pp.2400-2407.

Pizzi, A., Carrai, R., Falsini, C., Martini, M., Verdesca, S. and Grippo, A. (2009). Prognostic value of motor evoked potentials in motor function recovery of upper limb after stroke. *Journal of Rehabilitation Medicine*, 41(8), pp.654-660.

Pound, P., Bury, M. and Ebrahim, S. (1997). From apoplexy to stroke. *Age and Ageing*, 26(5), pp.331-337.

Prabhakaran, S., Zarahn, E., Riley, C., Speizer, A., Chong, J., Lazar, R., Marshall, R. and Krakauer, J. (2007). Inter-individual Variability in the Capacity for Motor Recovery After Ischemic Stroke. *Neurorehabilitation and Neural Repair*, 22(1), pp.64-71.

Puig J, Pedraza S, Blasco G et al. Acute damage to the posterior limb of the internal capsule on diffusion tensor tractography as an early imaging predictor of motor outcome after stroke. AJNR Am J Neuroradiol 2011; 32: 857–863. (2011).*Neuroradiologie Scan*, 1(01), pp.21-21.

Rondina, J., Park, C. and Ward, N. (2017). Brain regions important for recovery after severe post-stroke upper limb paresis. *Journal of Neurology, Neurosurgery & Psychiatry*, 88(9), pp.737-743.

Rossiter, H., Boudrias, M. and Ward, N. (2014). Do movement-related beta oscillations change after stroke?. *Journal of Neurophysiology*, 112(9), pp.2053-2058.

Rosso, C. and Samson, Y. (2014). The ischemic penumbra. *Current Opinion in Neurology*, 27(1), pp.35-41.

Sacco, R., Kasner, S., Broderick, J., Caplan, L., Connors, J., Culebras, A., Elkind, M., George, M., Hamdan, A., Higashida, R., Hoh, B., Janis, L., Kase, C., Kleindorfer, D., Lee, J., Moseley, M., Peterson, E., Turan, T., Valderrama, A. and Vinters, H. (2013). An Updated Definition of Stroke for the 21st Century. *Stroke*, 44(7), pp.2064-2089.

Schutta, S. (2009) Morgagni on apoplexy in De Sedibus: a historical perspective. *J Hist Neurosci*, pp.1– 24.

Schutta, S., Howe, M. (2006). Seventeenth century concepts of “apoplexy” as reflected in Bonet's “Sepulchretum”. *J Hist Neurosci*, pp.250–268.

Smith, M., Byblow, W., Barber, P. and Stinear, C. (2017). Proportional Recovery From Lower Limb Motor Impairment After Stroke. *Stroke*, 48(5), pp.1400-1403.

Song, M., Yu, S. (2014). Ionic Regulation of Cell Volume Changes and Cell Death after Ischemic Stroke. *Transl Stroke*, 5(1), pp.17–27.

Spalletti, C., Alia, C., Lai, S., Panarese, A., Conti, S., Micera, S. and Caleo, M. (2017). Combining robotic training and inactivation of the healthy hemisphere restores pre-stroke motor patterns in mice. *eLife*, 6.

Spalletti, C., Lai, S., Mainardi, M., Panarese, A., Ghionzoli, A., Alia, C., Gianfranceschi, L., Chisari, C., Micera, S. and Caleo, M. (2014). A robotic system for quantitative assessment and post-stroke training of forelimb retraction in mice. *Gait & Posture*, 40, p.S28.

Stinear, C. (2017). Prediction of motor recovery after stroke: advances in biomarkers. *The Lancet Neurology*, 16(10), pp.826-836.

Stinear, C., Barber, P., Petoe, M., Anwar, S. and Byblow, W. (2012). The PREP algorithm predicts potential for upper limb recovery after stroke. *Brain*, 135(8), pp.2527-2535.

Storey, C., Pols, H. (2009). Chapter 27 A history of cerebrovascular disease. *History of Neurology: Handbook of Clinical Neurology*, pp.401-415.

Stroemer, R., Kent, T. and Hulsebosch, C. (1993). Acute increase in expression of growth associated protein GAP-43 following cortical ischemia in rat. *Neuroscience Letters*, 162(1-2), pp.51-54.

Strokeeurope.eu. (2019). *The Burden of Stroke in Europe Report | King's College London for the Stroke Alliance for Europe*. [online] Available at: http://strokeeurope.eu/ [Accessed 23 Feb. 2019].

Strong, K., Mathers, C. and Bonita, R. (2007). Preventing stroke: saving lives around the world. *The Lancet Neurology*, 6(2), pp.182-187.

Stys, P. (2004). White Matter Injury Mechanisms. *Current Molecular Medicine*, 4(2), pp.113-130.

Takeuchi, N. and Izumi, S. (2012). Maladaptive Plasticity for Motor Recovery after Stroke: Mechanisms and Approaches. *Neural Plasticity*, 2012, pp.1-9.

Tamura, A., Graham, D., McCulloch, J. and Teasdale, G. (1981). Focal Cerebral Ischaemia in the Rat: 1. Description of Technique and Early Neuropathological Consequences following Middle Cerebral Artery Occlusion. *Journal of Cerebral Blood Flow & Metabolism*, 1(1), pp.53-60.

Tennant, K., Adkins, D., Donlan, N., Asay, A., Thomas, N., Kleim, J. and Jones, T. (2010). The Organization of the Forelimb Representation of the C57BL/6 Mouse Motor Cortex as Defined by Intracortical Microstimulation and Cytoarchitecture. *Cerebral Cortex*, 21(4), pp.865-876.

Traystman, R. (2003). Animal Models of Focal and Global Cerebral Ischemia. *ILAR Journal*, 44(2), p. 85-95.

User, S. (2019). *World Stroke Organization - World Stroke Organization*. [online] World-stroke.org. Available at: https://www.world-stroke.org/component/content/article/16-forpatients/84-facts-and-figures-about-stroke [Accessed 23 Feb. 2019].

Vallone, F., Lai, S., Spalletti, C., Panarese, A., Alia, C., Micera, S., Caleo, M. and Di Garbo, A. (2016). Post-Stroke Longitudinal Alterations of Inter-Hemispheric Correlation and Hemispheric Dominance in Mouse Pre-Motor Cortex. *PLOS ONE*, 11(1), p.e0146858.

Van Gijn, J., Kerr, R. and Rinkel, G. (2007). Subarachnoid haemorrhage. *The Lancet*, 369(9558), pp.306-318.

Wang, X., Liu, E., Wu, Z., Zhai, F., Zhu, Y., Shui, W. and Zhou, M. (2016). Skeleton-based cerebrovascular quantitative analysis. *BMC Medical Imaging*, 16(1).

Ward, N. (2003). Neural correlates of motor recovery after stroke: a longitudinal fMRI study. *Brain*, 126(11), pp.2476-2496.

Ward, N. (2017). Restoring brain function after stroke — bridging the gap between animals and humans. *Nature Reviews Neurology*, 13(4), pp.244-255.

Winters, C., Heymans, M., van Wegen, E. and Kwakkel, G. (2016). How to design clinical rehabilitation trials for the upper paretic limb early post stroke?. *Trials*, 17(1).

Winters, C., van Wegen, E., Daffertshofer, A. and Kwakkel, G. (2014). Generalizability of the Proportional Recovery Model for the Upper Extremity After an Ischemic Stroke. *Neurorehabilitation and Neural Repair*, 29(7), pp.614-622.

World Health Organization. (2019). *Global Health Estimates*. [online] Available at: https://www.who.int/healthinfo/global_burden_disease/en/ [Accessed 20 Feb. 2019].

Wu, J., Srinivasan, R., Burke Quinlan, E., Solodkin, A., Small, S. and Cramer, S. (2016). Utility of EEG measures of brain function in patients with acute stroke. *Journal of Neurophysiology*, 115(5), pp.2399-2405.

Xie, X., Atkins, E. and Lv, J. (2016). Effects of Intensive Blood Pressure Lowering on Cardiovascular and Renal Outcomes: Updated Systematic Review and Meta-Analysis. *Journal of Vascular Surgery*, 64(4), pp.1169-1170.

Yang, J., Mukda, S., Chen, S. (2018). Diverse roles of mitochondria in ischemic stroke. *Redox Biology*, pp.263–275.

Zeiler, S., Hubbard, R., Gibson, E., Zheng, T., Ng, K., O'Brien, R. and Krakauer, J. (2016). Paradoxical Motor Recovery From a First Stroke After Induction of a Second Stroke. *Neurorehabilitation and Neural Repair*, 30(8), pp.794-800.

Zemke, A., Heagerty, P., Lee, C. and Cramer, S. (2003). Motor Cortex Organization After Stroke Is Related to Side of Stroke and Level of Recovery. *Stroke*, 34(5).

Zhang, S., Ke, Z., Li, L., Yip, S. and Tong, K. (2013). EEG patterns from acute to chronic stroke phases in focal cerebral ischemic rats: correlations with functional recovery. *Physiological Measurement*, 34(4), pp.423-435.